

1. Publication N° <i>INPE-3625-RPI/136</i>	2. Version	3. Date <i>August, 1985</i>	5. Distribution <input checked="" type="checkbox"/> Internal <input type="checkbox"/> External <input type="checkbox"/> Restricted
4. Origin <i>DMC/DGC</i>	Program <i>CONTAT</i>		
6. Key words - selected by the author(s) <i>FLEXIBLE SPACECRAFT DYNAMICAL MODEL SPACECRAFT SIMULATIONS</i>			
7. U.D.C.: 629.7.062.2			
8. Title <i>SPINNER DYNAMICS FORMULATION</i>	10. Nº of pages: 83		
9. Authorship <i>Décio Castilho Ceballos</i> Responsible author <i>Décio Castilho</i>	11. Last page: 78		
12. Revised by  <i>Atair Rios Neto</i>		13. Authorized by  <i>Marco Antonio Raupp</i> Director General	
14. Abstract/Notes <i>This works presents a generalized dynamical model for a spin stabilized elastic spacecraft. The generalized coordinates, which include three coordinates related with the translational motion, three coordinates related with the rotational motion, and the coordinates related with the elastic modes, are imposed to satisfy the Lagrange's equation. The model is applied to simulate a simple idealized spacecraft. The results show the potential of having destabilizing influence on the controlled system due to appendage flexibility.</i>			
15. Remarks <i>This report was published in SPAR AEROSPACE in August, 1984 to present the research completed by Dr. Décio Castilho Ceballos when in a training on the job assignment at SPAR.</i>			

DISTRIBUTION LIST

Technical Memo No. **115**

DOC - 10 copies - H. Raine

M. Altmann

J.R.G. Cox

K. Duffy

L. Dyke - Original Set + 1

A. Kidd

G. Lewis

H. Moody

C. Morgan

J. Purchase

S. Sorocky

K. Spring

R. Subramaniam

L. Wegrowicz

J. Zacharatos

S. Nathan

Dr. Ceballos

N. Marinos

Distributed August 21, 1984.

PROJECT: M-SAT PHASE B

PROJECT NO: 5010-B

TECHNICAL MEMO: #115

SUBJECT: SPINNER DYNAMICS FORMULATION

GENERATED BY:

D. Ceballos
D. Ceballos - Resp. Eng.

EDITED BY:

N. Matlhos
N. Matlhos

DATE:

AUGUST 10, 1984

REVIEWED BY:

A. Kidd Aug 20, 1984
A. Kidd - Bus Supervisor

APPROVED BY:

G. Lewis Aug 20, 1984
G. Lewis - Systems Manager

C. Morgan Aug 21/84
C. Morgan - Program Manager

Spar Aerospace Limited
21025 Trans-Canada Highway
Ste-Anne-de-Bellevue, Quebec
Canada H9X 3R2



TABLE OF CONTENTS

1. Preface/Introduction/References
2. Generalized State Coordinate Model
 - 2.1 General Considerations
 - 2.2 Basic Attitude Model
 - 2.3 Basic Translation and Attitude Model
 - 2.4 Inclusion of Elastic Displacement Effect of Point P Velocity
 - 2.3.1 The Contribution of the L_{41} Term
 - 2.3.2 The Contribution of the L_{42} Term
 - 2.3.3 The Contribution of the L_{43} Term
 - 2.3.4. The Contribution of the L_{44} Term
3. The Numerical Modelling and Simulation of a Simple Idealized Spacecraft.
 - 3.1 Linear Time Invariant Attitude Dynamic Model
 - 3.2 Linear Model for the Idealized Spacecraft
 - 3.3 Evaluation Model
 - 3.4 Control of the Despun Platform
 - 3.5 Simulation Results
4. Conclusion
5. Appendix A, Simulation Plots

PREFACE

This technical memo is intended to present the research completed by Dr. D. Ceballos currently working for Spar on visit from INPE.

REFERENCES:

1. Bryson Jr., A.E.: Ho, Y.C., Applied Optimal Control, New York, John Wiley, 1975.
2. Hughes, P.C., Coordinate Alternatives for Flexible Spacecraft Dynamics Analysis. DOC-SR-SP-83-049, Ontario Dynacon, 1983.
3. Jazwinski, A.H., Stochastic Process and Filter Theory, New York, Academic, 1970.
4. Meirovich, L., Methods of Analytical Dynamics, New York, McGraw Hill, 1970.
5. West-Vukovich, G., Structural Dynamics Model for a Harris-Like Antenna Reflector, DOC-CR-SP-84-006, Ontario, Dynacon, 1984.

1. INTRODUCTION

Problems associated with the dynamics and control of satellite systems can be divided into two intimately related broad classes, the first involving modelling and the second, computational aspects.

The modelling problems arise from the fact that for complicated structures, the dynamic characteristics such as the S/C natural frequencies and modes, cannot be determined with the same accuracy as for simple structures (such as uniform beams or membranes) since numerical analysis techniques must be used due to the absence of a closed form solution to the eigenvalue problem. Truncation, implied by the use of numerical analysis techniques has a profound effect on the computed natural modes particularly on the higher ones, so that one must distinguish between computed and actual natural frequencies and modes. Because computed lower modes tend to approach the actual ones as the order of the mathematical model is increased, it follows that a good simulation must be of sufficiently high order to permit accurate determination of the S/C modes to be controlled.

The second class of problems arises because of the computational difficulties inherent in the application of various control algorithms to higher order systems.

The numerical values (parameters for a specific S/C) required for the dynamic model for complex S/C normally cannot be obtained in laboratory tests. Sufficient approximations of these values can be obtained in the use of finite element techniques (such as NASTRAN).

The objective of this report is to present a generalized dynamic model of a spin-stabilized S/C with flexible appendages. A simple idealized S/C is considered as an example.

2. GENERALIZED STATE COORDINATE MODEL

2.1 General Considerations

Consider a flexible spinning body (see fig. 2-1) consisting of a central rigid body (CR), a spinning rigid rotor (SR) and a number of elastic appendages (EA).

For simplicity, we focus attention on a single generalized flexible appendage, however, all appendages can be included by summation.

The Lagrange's equations of motion for the n-generalized coordinates q_k ($k=1,2,\dots,n$) can be written in the matrix form.

$$\frac{d}{dt} \left[\begin{matrix} \frac{\partial L}{\partial \dot{q}_k} \end{matrix} \right] - \left[\begin{matrix} \frac{\partial L}{\partial q_k} \end{matrix} \right] = [Q] \quad (2.1) \quad \text{where } L = T - V \quad (2.2)$$

Where q_k are the generalized coordinates, T and V are the kinetic and potential energies respectively and Q_k are the non-potential forces.

The generalized coordinate may be subdivided into

$$\vec{q} = \begin{vmatrix} \vec{q}_T \\ \vec{q}_R \\ \vec{q}_E \end{vmatrix} \quad (2.3)$$

Where the \vec{q}_T vector contains three generalized coordinates related with the translational motion of coordinate systems, the \vec{q}_R vector contains three generalized coordinates related with the rotational motion of coordinate systems and \vec{q}_E is a generalized coordinate vector related with the elastic modes.

$$\text{We have } \vec{q} = \begin{vmatrix} x \\ y \\ z \end{vmatrix} \quad (2.4), \quad \vec{q} = \begin{vmatrix} \theta_x \\ \theta_y \\ \theta_z \end{vmatrix} \quad (2.5)$$

$$\text{and } \dot{\vec{\theta}} = \vec{\omega} = \begin{vmatrix} \omega_x \\ \omega_y \\ \omega_z \end{vmatrix} \quad (2.6)$$

where the rotor revolves about the Z-axis.

2.1 (cont'd)

The generalized position of the spacecraft can be defined by

$$\mathbf{P} = \mathbf{O} + \sum_i P_i \mathbf{q}_i \quad (2.7)$$

where O is the coordinate system origin, P_i is the coordinate of the point P in the spacecraft and \mathbf{q}_i is the displacement of P due to the generalized coordinate q_{Ei} corresponding to the ith elastic mode.

The velocity of the point P is defined by

$$\frac{d(\mathbf{P})}{dt} = \dot{\mathbf{q}} + \sum_i \dot{P}_i \mathbf{q}_i + \omega \times [\mathbf{P} + \sum_i P_i \mathbf{q}_i] \quad (2.8)$$

$$\text{or } \frac{d\mathbf{P}}{dt} = \dot{\mathbf{q}} + \sum_i \dot{P}_i \mathbf{q}_i - \mathbf{P} \omega - \sum_i P_i \omega \mathbf{q}_i \quad (2.9)$$

$$\mathbf{P}_s^* = \begin{vmatrix} 0 & -P_z & P_y \\ S & S & S \\ z & x & x \\ P & 0 & -P \\ S & S & S \\ y & x & x \\ -P & P & 0 \\ S & S & S \end{vmatrix} \quad (2.10) \quad \mathbf{x}_i^* = \begin{vmatrix} 0 & -x_z & x_y \\ i & i & i \\ z & 0 & -x \\ x & i & i \\ y & x & x \\ -x & x & 0 \\ i & i & i \end{vmatrix} \quad (2.11)$$

The kinetic energy can now be written as:

$$T = \frac{1}{2} \int_{\text{SPACECRAFT}} \left[\dot{\mathbf{q}}_T + \sum_i \dot{P}_i \mathbf{q}_i^* - \sum_i P_i \dot{\theta}_i - \sum_i \dot{\theta}_i \mathbf{q}_i^* \right]^T \left[\dot{\mathbf{q}}_T + \sum_i \dot{P}_i \mathbf{q}_i^* - \sum_i P_i \dot{\theta}_i - \sum_i \dot{\theta}_i \mathbf{q}_i^* \right] dm + I_z \Omega_z^2 + \frac{1}{2} I_z \Omega_z^2 \quad (2.12)$$

where Ω represents the angular velocity of the spinning section.

2.1 (cont'd)

$$\text{or } T = \frac{1}{2} \begin{vmatrix} \dot{q}_T \\ \dot{\theta} \\ \dot{q}_{Ei} \\ \dot{\theta} q_{Ei} \end{vmatrix}^T \cdot \left[\begin{array}{cccc} 1 & -P_s^* & X_j & -X_j^* \\ P_s^* & -P_s^* P_s & P_s^* X_j & -P_s^* X_j^* \\ X_i^T & -X_i^T P_s^* & -X_i^T X_j & -X_i^T X_j^* \\ X_i^* & -X_i^* P_s^* & -X_i^* X_j & -X_i^* X_j^* \end{array} \right] dm \cdot \begin{vmatrix} \dot{q}_T \\ \dot{\theta} \\ \dot{q}_{Ej} \\ \dot{\theta} q_{Ej} \end{vmatrix}$$

Spacecraft

$$+ I_z^R \Omega \omega_z + \frac{1}{2} I_z^R \Omega^2 \quad (2.13)$$

$$\text{or } T = \frac{1}{2} \begin{vmatrix} \dot{q}_T \\ \dot{\theta} \\ \dot{q}_{Ei} \\ \dot{\theta} q_{Ei} \end{vmatrix}^T \cdot \begin{bmatrix} m_{11} & m_{12} & m_{13}^i & m_{14}^j \\ m_{21} & m_{22} & m_{23}^i & m_{24}^j \\ m_{31}^i & m_{32}^i & m_{33}^{ij} & m_{34}^{ij} \\ m_{41}^i & m_{42}^i & m_{43}^{ij} & m_{44}^{ij} \end{bmatrix} \cdot \begin{vmatrix} \dot{q}_T \\ \dot{\theta} \\ \dot{q}_{Ej} \\ \dot{\theta} q_{Ej} \end{vmatrix} + I_z^R \Omega \omega_z + \frac{1}{2} I_z^R \Omega^2 \quad (2.14)$$

$$\text{where } m_{11} = [1]_m \quad (2.15)$$

$$m_{21} = m_{12}^T = \int_{\text{SPACECRAFT}} P_s^* dm \quad (2.16)$$

$$[m_{31}^i]^T = m_{13}^i = \int_{\text{FLEXIBLE APPENDAGE}} X_i dm \quad (2.17)$$

$$m_{41}^i = [m_{14}^j]^T = \int_{\text{FLEXIBLE APPENDAGE}} X_i^* dm \quad (2.18)$$

$$m_{22} = \int_{\text{SPACECRAFT}} -P_s^* P_s^* dm \quad (2.19)$$

$$[m_{32}^i]^T = m_{23}^i = \int_{\text{FLEXIBLE APPENDAGE}} P_s^* X_i dm \quad (2.20)$$

2.1 (cont'd)

$$M_{42}^i = [m_{24}^i]^T = \int_{\text{FLEXIBLE APPENDAGE}} -X_i^* P_s^* dm \quad (2.21)$$

$$M_{33}^{ij} = \int_{\text{FLEXIBLE APPENDAGE}} X_i^T X_j dm \quad (2.22)$$

$$M_{43}^{ij} = [m_{34}^{ij}]^T = \int_{\text{FLEXIBLE APPENDAGE}} X_i^* X_j dm \quad (2.23)$$

$$M_{44}^{ij} = \int_{\text{FLEXIBLE APPENDAGE}} -X_i^* X_j^* dm \quad (2.24)$$

The potential energy can arise from various sources, such as gravity and body elasticity. The potential energy of the elastic spacecraft can be simplified to a form due entirely from elastic effects (since the elastic potential is dominant) and can be written in the general form as:

$$V = \frac{1}{2} q_E^T \bar{K}_{ij} q_E \quad (2.25)$$

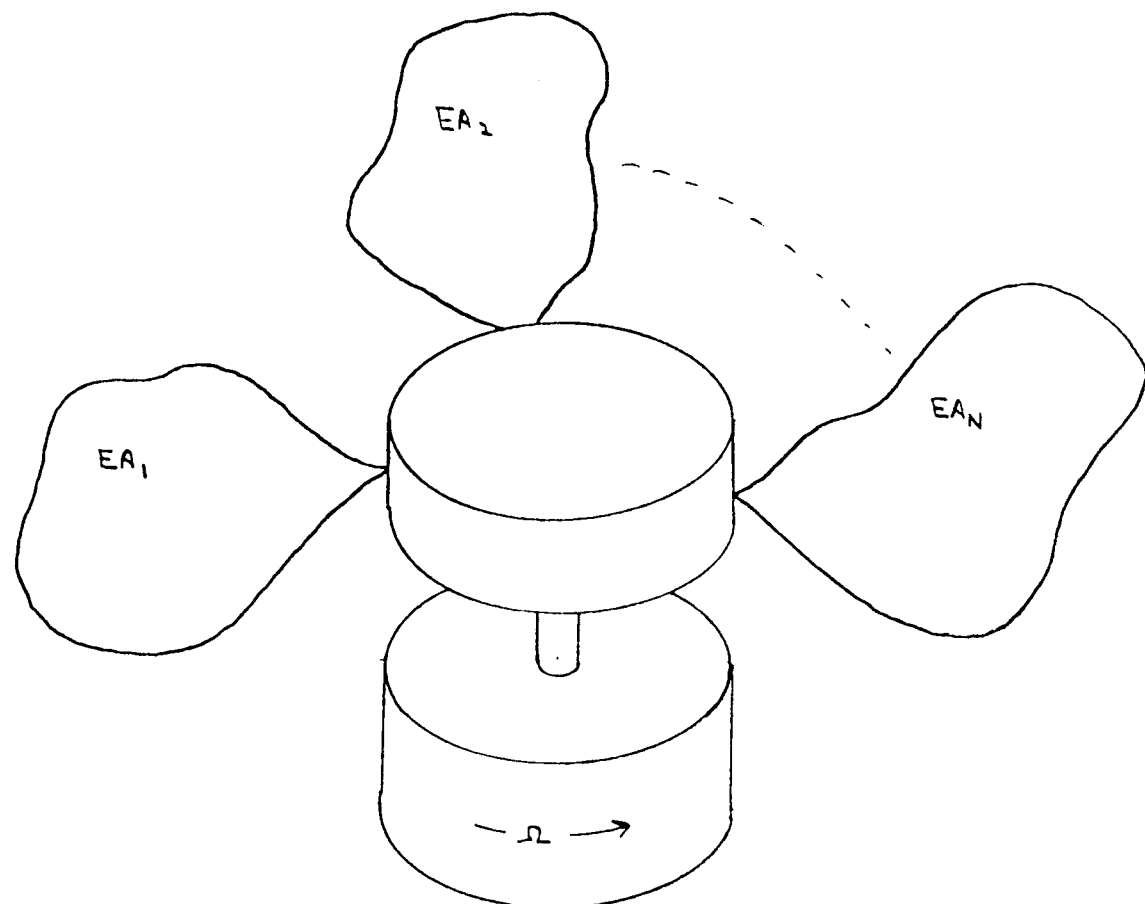
$$\text{where } \bar{K}_{ij} = \int_{\text{FLEXIBLE APPENDAGE}} X_i^T A_D X_j dD + \int_{\text{FLEXIBLE APPENDAGE}} X_i^T A_S X_j dS \quad (2.26)$$

Where D represents the integration domain and S its boundaries, A_S and A_D are positive-symmetric energy matrices.

The derivation of the global dynamic equation is easy but tedious work. This derivation would evolve simply by the direct application of the Lagrangian equation, however, the model derived in this form would be difficult to handle.

The generalized model must be manageable otherwise it would not have many applications. Normally, only parts of the generalized model are used. The generalized model is derived in steps, starting by creating a linear attitude model and then including the translation coordinates and coupling effects.

FIGURE 2.1 DUAL SPIN SPACECRAFT WITH FLEXIBLE APPENDAGES



2.2 Basic Attitude Model

The translational and elastic displacement effects and a point P_e velocity are not included at this stage for the basic model.

The Lagrangian equation is then

$$L_{\text{BASIC ATTITUDE}} = \frac{1}{2} \dot{\theta}^T M_{22} \dot{\theta} + \frac{1}{2} \dot{\theta}^T M_{23} q_{Ej} + \frac{1}{2} \dot{q}_{Ei} M_{32}^i \dot{\theta} + \frac{1}{2} \dot{q}_{Ei} M_{33}^{ij} \dot{q}_{Ej} \checkmark \\ + I_z^R \Omega \dot{\theta}_z + \frac{1}{2} I_z^R \Omega^2 - \frac{1}{2} q_{Ei} K_{ij} q_{Ej} \quad (2.27)$$

The Langrange's equation (Eq 2.1) for θ applied to the Lagrangian equation (2.27) result in,

$$m_{22} \ddot{\theta} + \dot{\theta}^* m_{22} \dot{\theta} + I_z^R \begin{vmatrix} \Omega \dot{\theta}_y \\ -\Omega \dot{\theta}_x \\ \Omega \end{vmatrix} + m_{23}^{ij} \ddot{q}_{Ej} + \dot{\theta}^* m_{23}^{ij} q_{Ej} = Q_2 \quad (2.28)$$

where

$$\dot{\theta}^* = \begin{vmatrix} 0 & -\dot{\theta}_z & \dot{\theta}_y \\ \dot{\theta}_z & 0 & -\dot{\theta}_x \\ -\dot{\theta}_y & \dot{\theta}_x & 0 \end{vmatrix} \quad (2.29)$$

and

$$m_{33}^{ij} \ddot{q}_{Ej} + \dot{\theta}^* m_{33}^{ij} q_{Ej} + K_{ij} q_{Ej} + m_{32}^i \ddot{\theta} + \dot{\theta}^* m_{32}^i \dot{\theta} = Q_3 \quad (2.30)$$

We have an additional relationship associated with coupling torque:

$$I_z^R (\dot{\omega}_z + \dot{\Omega}) = T \quad (2.31)$$

where T is the torque magnitude applied to the rotor axis.

2.3 Basic Translation and Attitude Model

The Lagrangian of the translation and attitude model will include the following translational terms:

$$L_{11} = \frac{1}{2} \dot{q}_T^T M_{11} \dot{q}_T \quad (2.32)$$

$$L_{21} = \frac{1}{2} \dot{\Theta}^T M_{21} \dot{q}_T + \frac{1}{2} \dot{q}_T^T M_{12} \dot{\Theta} \quad (2.33)$$

$$L_{31} = \frac{1}{2} \dot{q}_{Ei}^T M_{31}^i \dot{q}_T + \frac{1}{2} \dot{q}_T^T M_{13}^j \dot{q}_{Ei} \quad (2.34)$$

Using the Lagrangian defined by eqn 2.27, we can define a new Lagrangian by

$$L_{\substack{\text{BASIC ATTITUDE} \\ \downarrow \text{TRANSLATION}}} = L_{\substack{\text{BASIC} \\ \text{ATTITUDE}}} + L_{11} + L_{21} + L_{31} \quad (2.35)$$

and applying the Lagrange's equation (Eqn 2.1) for to the new Lagrangian (2.35) results to the following:

$$m_{11} \ddot{q}_T + \dot{\Theta}^* m_{11} \dot{q}_T + P_{21}^{q_T} + P_{31}^{q_T} = Q_1 \quad (2.36)$$

where the $P_{21}^{q_T}$ and $P_{31}^{q_T}$ terms are due to the contribution of the L_{21} and L_{31} terms respectively (eqn 2.35).

$$P_{21}^{q_T} = m_{12} \ddot{\Theta} + \dot{\Theta}^* m_{12} \dot{\Theta} \quad (2.37)$$

and

$$P_{31}^{q_T} = m_{13}^i \ddot{q}_{Ei} + \dot{\Theta}^* m_{13}^i \dot{q}_{Ei} \quad (2.38)$$

2.3 (cont'd)

Applying Lagrange's equation (2.1) for Θ to the Lagrangian (eqn. 2.35) similarly results to equation 2.28 with an additional term P_{21}^Θ associated with L_{21} added to the left hand side. P_{21}^Θ is given as follows:

$$P_{21}^\Theta = M_{21}\ddot{q}_\tau + \dot{\Theta}^* M_{21}\dot{q}_\tau \quad (2.39)$$

We also have

$$P_{11}^\Theta = 0 \text{ and } P_{31}^\Theta = 0$$

Applying Lagrange's equation (2.1) for $q_{\epsilon i}$ to the Lagrangian (eqn 2.35) similarly results to equation 2.30 with an additional term $P_{31}^{q_{\epsilon i}}$ associated with L_{31} added to the left hand side. $P_{31}^{q_{\epsilon i}}$ is given as follows,

$$P_{31}^{q_{\epsilon i}} = M_{31}^i\ddot{q}_\tau + \dot{\Theta}^* M_{31}^i\dot{q}_\tau \quad (2.40)$$

We also have $P_{11}^{q_{\epsilon i}} = 0$ and $P_{21}^{q_{\epsilon i}} = 0$.

2.4 Inclusion of Elastic Displacement Effect on the Point P Velocity

The term ($-x^* q_{\epsilon i} \omega$) found in equation 2.9 represents the effect of displacement $q_{\epsilon i}$ on the point P velocity of the spacecraft. In the kinetic energy expression (2.14), this term is weighted by the elements found in the fourth row of matrix M (eqn. 2.14) and the corresponding transposes,

$$\text{ie: } m_{41}^i, m_{14}^j, m_{42}^i, m_{24}^j, m_{43}^{ij}, m_{34}^{ij}, m_{44}^{ij}$$

The Lagrangian's corresponding to the above elements (submatrices) are given by,

$$L_{41} = \frac{1}{2} q_{\epsilon i} \dot{\theta}^T m_{41}^i \dot{q}_T + \frac{1}{2} \dot{q}_T^T m_{14}^j q_{\epsilon j} \dot{\theta} \quad (2.41)$$

$$L_{42} = \frac{1}{2} q_{\epsilon i} \dot{\theta}^T m_{42}^i \dot{\theta} + \frac{1}{2} \dot{\theta}^T m_{24}^j q_{\epsilon j} \dot{\theta} \quad (2.42)$$

$$L_{43} = \frac{1}{2} q_{\epsilon i} \dot{\theta}^T m_{43}^{ij} \dot{q}_{\epsilon j} + \frac{1}{2} \dot{q}_{\epsilon i}^T m_{34}^{ij} q_{\epsilon j} \dot{\theta} \quad (2.43)$$

$$L_{44} = \frac{1}{2} q_{\epsilon i} \dot{\theta}^T m_{44}^{ij} q_{\epsilon j} \dot{\theta} \quad (2.44)$$

2.4.1 The Contribution of the L₄₁ Term

Applying the Lagrange's equation (2.1) for Θ to the Lagrangian (eqn 2.41) L_{41} results to:

$$P_{41}^{\Theta} = \dot{q}_{\epsilon i} m_{41}^i \dot{q}_T + q_{\epsilon i} m_{41}^i \ddot{q}_T + \dot{\Theta}^* q_{\epsilon i} m_{41}^i \dot{q}_T \quad (2.45)$$

Similarly, by applying Lagrange's equation (2.1) for $q_{\epsilon i}$ and then for q_T to L_{41} results to the following equations resp.:

$$P_{41}^{q_{\epsilon i}} = -\dot{\Theta}^* m_{41}^i \dot{q}_T, \text{ for } q_{\epsilon i} \quad (2.46)$$

and

$$P_{41}^{q_T} = m_{41}^i \ddot{\Theta} q_{\epsilon i} + m_{41}^i \dot{\Theta} \dot{q}_{\epsilon i} + \dot{\Theta}^* m_{41}^i \dot{\Theta} q_{\epsilon i}, \text{ for } q_T \quad (2.47)$$

2.4.2 The Contribution of the L42 Term

Applying the Lagrange's equation (2.1) for Θ to the Lagrangian (eqn. 2.42) L_{42} results to:

$$P_{42}^{\Theta} = m_{42}^i \dot{\Theta} \dot{q}_{\epsilon i} + m_{42}^i \ddot{\Theta} q_{\epsilon i} + \dot{\Theta}^* m_{42}^i \ddot{\Theta} q_{\epsilon i} \quad (2.48)$$

Similarly, by applying Lagrange's equation (2.1) for $q_{\epsilon i}$ and then for q_T to L_{42} results to the following equations, resp. :

$$P_{42}^{q_{\epsilon i}} = -\dot{\Theta}^T m_{42}^i \dot{\Theta} \quad , \text{for } q_{\epsilon i} \quad (2.49)$$

and

$$P_{42}^{q_T} = 0 \quad , \text{for } q_T \quad (2.50)$$

2.4.3 The Contribution of the L43 Term

Similarly, as obtained in the previous section, the application of Lagrange's equation (2.1) for Θ , $q_{\epsilon i}$ and q_T to the Lagrangian L 43 result to:

$$P_{43}^{\Theta} \equiv M_{43}^{ij} \dot{q}_{\epsilon i} \dot{q}_{\epsilon j} + M_{43}^{ij} q_{\epsilon i} \ddot{q}_{\epsilon j} + \dot{\Theta}^* M_{43}^{ij} q_{\epsilon i} \dot{q}_{\epsilon j}, \text{ for } \Theta \quad (2.51)$$

$$P_{43}^{q_{\epsilon i}} \equiv M_{34}^{ij} \ddot{\Theta} q_{\epsilon j} + \dot{\Theta}^* M_{34}^{ij} \dot{\Theta} q_{\epsilon j}, \text{ for } q_{\epsilon i} \quad (2.52)$$

and $P_{43}^{q_T} \equiv 0$, for q_T (2.53)

2.4.4 The Contribution of the L44 Term

The application of the Lagrange's equation (2.1) for θ, q_{Ei} and q_T to the Lagrangian L44 result to:

$$P_{44}^{\theta} = M_{44}^{ij} \ddot{\theta} q_{Ei} q_{Ej} + 2 M_{44}^{ij} \dot{\theta} \dot{q}_{Ei} q_{Ej} + \dot{\theta}^* M_{44}^{ij} \dot{\theta} q_{Ei} q_{Ej} - \dot{\theta}^T M_{44}^{ij} \dot{\theta} q_{Ei} q_{Ej}, \text{ for } \theta \quad (2.54)$$

$$P_{44}^{q_{Ei}} = -\dot{\theta}^T M_{44}^{ij} \dot{\theta} q_{Ei}, \text{ for } q_{Ei} \quad (2.55)$$

$$\text{and } P_{44}^{q_T} = 0 \quad \text{for } q_T \quad (2.56)$$

3. THE NUMERICAL MODELLING AND SIMULATION OF A SIMPLE IDEALIZED SPACECRAFT

A realistic numerical model for the M-SAT satellite is impossible to obtain at this point due to insufficient information. An idealized vehicle is devised to permit preliminary analysis. Simulations are realized to provide a preliminary feeling about the interaction between rotation and elasticity.

Only attitude motion, small Θ and constant rotation of the spinning section are considered for the simplified idealized model. Two dipole-like elementary elastic appendages are considered for the model.

3.1 Linear Time Invariant Attitude Dynamic Model

Considering attitude motion only, small Θ , constant angular velocity Ω of spinning body, the non-potential forces Q_2 and Q_3 are given by:

$$Q_2 = B_R u ; \quad (3.1)$$

$$Q_3 = -g_E q_{\epsilon j} + B_{\epsilon i} u \quad (3.2)$$

where u is the control vector. The linear time invariant model can be given by:

$$m_{22}\ddot{\Theta} + m_{23}\ddot{q}_{\epsilon i} + g_{RR}\dot{\Theta} = B_R u , \quad (3.3)$$

$$m_{32}\ddot{\Theta} + m_{33}\ddot{q}_{\epsilon j} + g_E \dot{q}_{\epsilon j} + K_E q_{\epsilon j} = B_{\epsilon i} u , \quad (3.4)$$

where $g_{RR} = \begin{vmatrix} 0 & \Omega I_z^R & 0 \\ -\Omega I_z^R & 0 & 0 \\ 0 & 0 & 0 \end{vmatrix} ; \quad (3.5)$

Or in another form, the model can be given by,

$$M\ddot{q} + g\dot{q} + kq = Bu ; \quad (3.6)$$

Equation 3.6 represents the equation of motion for our simplified vehicle where M , g , k represent the mass, damping and stiffness matrices respectively.

3.1 (cont'd)

$$\text{Where } M = \begin{vmatrix} m_{22} & m_{23}^j \\ m_{31}^i & m_{33}^{ij} \end{vmatrix} \quad (3.7)$$

$$g = \begin{vmatrix} g_{RR} & 0 \\ 0 & g_E^{ij} \end{vmatrix} \quad (3.8)$$

$$k = \begin{vmatrix} 0 & 0 \\ 0 & K_E^{ij} \end{vmatrix} \quad (3.9)$$

$$B = \begin{vmatrix} B_R \\ B_E^i \end{vmatrix} \quad (3.10)$$

The modal coordinates associated with cantelevered elastic appendages are often used in hybrid coordinate models. The equations of motion for elastic appendages can be written as,

$$[m_{33}^{ij}] \ddot{q}_E + [g_E^{ij}] \dot{q}_E + [K_E^{ij}] q_E = [B_E^i] u ; \quad (3.11)$$

Also, $[g_E^{ij}]$ is given by,

$$[g_E^{ij}] = 2c_a [m_{33}^{ij}]^{1/2} \cdot [\sigma_{Ei}^2] \cdot [m_{33}^{ij}]^{1/2} ; \quad (3.12)$$

where σ_{Ei} is an undamped elastic vibration mode and c_a is a damping coefficient.

The K_E^{ij} submatrix can be decoupled by performing the following transformation.

3.1 (cont'd)

$$P_E^T [M_{33}^{ij}] P_E = I \quad ; \quad (3.13)$$

$$P_E^T [K_E^{ij}] P_E = \text{Diag} [\sigma_{Ei}^2] \quad ; \quad (3.14)$$

$$P_E^T [g_E^{ij}] P_E = 2C_0 \cdot \text{Diag} [\sigma_{Ei}] \quad ; \quad (3.15)$$

Where P_E can be obtained by solving the eigenvalue problem for the undamped system,

$$[[K_E^{ij}] - \sigma_{Ei}^2 [M_{33}^{ij}]] \omega = 0 \quad ; \quad (3.16)$$

And

$$P_E = [\omega_1, \omega_2, \dots, \omega_N] \cdot N \quad ; \quad (3.17)$$

where ω_k are the eigenvectors and N is the diagonal matrix defined by

$$N_{ii} = \omega_{1i}^{-\gamma_2} \quad ; \quad (3.18)$$

where

$$\omega = [\omega_i]^T \cdot [M_{33}^{ij}] \omega_i \quad ; \quad (3.19)$$

The eigenvalues equations can be solved by computer program. The hybrid coordinate system derived from the linear time invariant model equations 3.3 through 3.5 using the abovementioned transformations can be shown to be:

$$m_{22} \ddot{\theta} + \bar{m}_{23}^i \ddot{\Delta}_i + g_{Rk} \dot{\theta} = B_R u \quad ; \quad (3.20)$$

$$\bar{m}_{32}^i \ddot{\theta} + \ddot{\Delta}_i + 2C_0 \sigma_{Ei} \dot{\Delta}_i + \sigma_{Ei}^2 \Delta_i = \bar{B}_E u \quad ; \quad (3.21)$$

where Δ_i is the modal coordinate and the modified matrices are defined as follows:

$$[\bar{m}_{23}^i]^T = [\bar{m}_{32}^i] = P_E^T [M_{32}^i] \quad ; \quad (3.22)$$

$$\text{and } [\bar{B}_E^i] = P_E^T [B_E^i] \quad ; \quad (3.23)$$

FIGURE 3-1 IDEALIZED SPACECRAFT

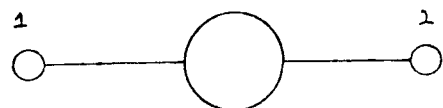
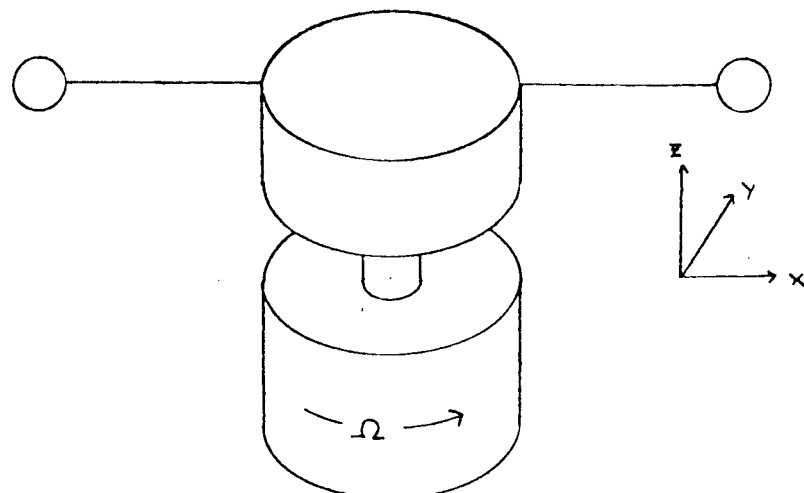


Figure 3-2 Two Nodes

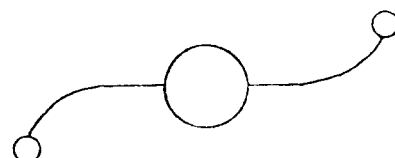


Figure 3-3 First Mode Shape

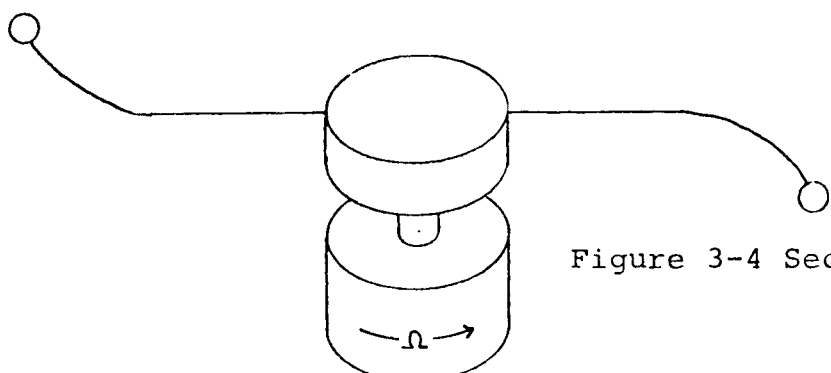


Figure 3-4 Second Mode Shape

3.2 Linear Model for the Idealized Spacecraft

The objective of this section is to define the values for the numerical parameters to be used in the preliminary digital simulations. A simple idealized spacecraft illustrated in Fig. 3-1 is devised to permit a physically meaningful analysis.

The idealized spacecraft includes two elastic appendages attached to a rigid body. The rigid body is attached to a rigid symmetric rotor spinning at Ω angular velocity. The elastic appendages each of length L are massless except for a tip mass 'm' at each end.

Beam stiffness is chosen such that we obtain the beams natural frequencies ϵ_x and ϵ_y in the Z - X and Y - X planes respectively (see figures 3-3 and 3-4). The free translational motion establishes some symmetrical mode shapes with corresponding natural frequencies. However, if the spacecraft body dimensions are considered small with respect to the appendage length, these mode shapes can be neglected. The mode shapes due only to attitude motion are illustrated schematically in figures 3-2 to 3-4.

3.2 (cont'd)

Assuming that the spacecraft's dimensions are small with respect to the appendage length L and the coordinate system is centered on the spacecraft, the submatrices $M_{32}^i, M_{23}^i, M_{13}^i$ can be defined as functions of m and L

Recalling that Equation 2-20 was used to obtain M_{32}^i and M_{23}^i we have,

$$[M_{32}^i]^T = M_{23}^i = \int_{\text{flexible Appendage}} P_s^* X_i dm ; \quad (3.24)$$

For the first mode shape and the first node, P_{S1}^* , X_{11} and $P_{S1}^* X_{11}$ are given by

$$P_{S1}^* = \begin{vmatrix} 0 & 0 & 0 \\ 0 & 0 & L \\ 0 & -L & 0 \end{vmatrix} ; \quad (3.25)$$

$$X_{11} = \begin{vmatrix} 0 \\ L \\ 0 \end{vmatrix} ; \quad (3.26)$$

$$\text{and } P_{S1}^* X_{11} = \begin{vmatrix} 0 \\ 0 \\ -L^2 \end{vmatrix} ; \quad (3.27)$$

For the first mode shape and the second node, P_{S2}^* , X_{12} and $P_{S2}^* X_{12}$ are given by

$$P_{S2}^* = \begin{vmatrix} 0 & 0 & 0 \\ 0 & 0 & -L \\ 0 & L & 0 \end{vmatrix} ; \quad (3.28)$$

$$X_{12} = \begin{vmatrix} 0 \\ -L \\ 0 \end{vmatrix} ; \quad (3.29)$$

3.2 (Cont'd)

$$\text{and } P_{S2}^* X_{12} = \begin{vmatrix} 0 \\ 0 \\ -L^2 \end{vmatrix} ; \quad (3.30)$$

$$\text{Then } [m_{32}^1]^T = m_{23}^1 = 2m \begin{vmatrix} 0 \\ 0 \\ -L^2 \end{vmatrix} ; \quad (3.31)$$

Similarly, for the second mode shape and the first node we have:

$$X_{21} = \begin{vmatrix} 0 \\ 0 \\ L \end{vmatrix} ; \quad (3.32) \quad , \quad P_{S1}^* X_{21} = \begin{vmatrix} 0 \\ L^2 \\ 0 \end{vmatrix} ; \quad (3.33)$$

And for the second mode shape and the second node ,

$$X_{22} = \begin{vmatrix} 0 \\ 0 \\ -L \end{vmatrix} ; \quad (3.34) \quad , \quad P_{S2}^* X_{22} = \begin{vmatrix} 0 \\ L^2 \\ 0 \end{vmatrix} ; \quad (3.35)$$

and

$$[m_{32}^2]^T = m_{23}^2 = 2m \begin{vmatrix} 0 \\ L^2 \\ 0 \end{vmatrix} ; \quad (3.36)$$

3.2 (Cont'd)

Equation 2.22 is used to obtain M_{33}^{ij} ,

$$M_{33}^{ij} = \int_{\text{flexible spacecraft}} X_i^T X_j dm ; \quad (3.37)$$

$$M_{33}^{11} = 2mL^2 ; \quad (3.38)$$

$$M_{33}^{12} = M_{33}^{21} = 0 ; \quad (3.39)$$

$$M_{33}^{22} = 2mL^2 ; \quad (3.40)$$

The transformation matrix P_E must now be obtained. Having solved the M_{33}^{ij} submatrix, we can easily obtain P_E using equation 3.13 (since M_{33}^{ij} is diagonal). P_E is found to be,

$$P_E = \begin{vmatrix} \frac{1}{\sqrt{2m}L} & 0 \\ 0 & \frac{1}{\sqrt{2m}L} \end{vmatrix} ; \quad (3.41)$$

And the modified mass matrices, \bar{M}_{32}^{ij} and \bar{M}_{23}^{ij} are solved using equation 3.22, and are given by:

$$[\bar{M}_{32}^{1}]^T = \bar{M}_{23}^{1} = \sqrt{2m} \begin{vmatrix} 0 \\ 0 \\ -L \end{vmatrix} ; \quad (3.42)$$

$$[\bar{M}_{32}^{2}]^T = \bar{M}_{23}^{2} = \sqrt{2m} \begin{vmatrix} 0 \\ L \\ 0 \end{vmatrix} ; \quad (3.43)$$

3.4 (Cont'd)

The equations corresponding to the previously derived hybrid coordinate system equations 3.20 and 3.21 are given by:

$$M_{zz} \ddot{\Theta} + \begin{vmatrix} 0 & & \\ \sqrt{2m} L \cdot \dot{\delta}_2 & \ddots & \\ & \ddots & \sqrt{2m} L \cdot \dot{\delta}_1 \end{vmatrix} + g_{RR} \dot{\Theta} = B_R u ; \quad (3.44)$$

$$\text{and } \begin{vmatrix} -L \sqrt{2m} \ddot{\Theta}_z & & \\ & L \sqrt{2m} \ddot{\Theta}_y & \end{vmatrix} + \ddot{\lambda} + 2c_0 [\epsilon_{Ei}] \dot{\lambda} + [\epsilon_{Ei}^2] \lambda = \bar{B}_{Ei} u ; \quad (3.45)$$

The above equations can be rewritten in a simplified form

$$\bar{M} \ddot{r} + \bar{g} \dot{r} + \bar{k} r = \bar{B} u ; \quad (3.46)$$

Where

$$\bar{M} = \begin{vmatrix} J_x & J_{xy} & J_{xz} & 0 & 0 \\ J_{yx} & J_y & J_{yz} & 0 & C_1 \\ J_{zx} & J_{zy} & J_z & C_2 & 0 \\ 0 & 0 & C_2 & 1 & 0 \\ 0 & C_1 & 0 & 0 & 1 \end{vmatrix} ; \quad (3.47)$$

$$\text{where } C_1 = \sqrt{2m} \cdot L ; \quad (3.48) \text{ and } C_2 = -\sqrt{2m} \cdot L ; \quad (3.49)$$

$$\text{and } J_x = J_{zz} + J_{yy} ; \quad (3.50)$$

$$J_y = J_{xx} + J_{zz} ; \quad (3.51)$$

$$J_z = J_{xx} + J_{yy} ; \quad (3.52)$$

3.2 (Cont'd)

$$\bar{D} = \begin{vmatrix} 0 & I_2^T \Omega & 0 & 0 & 0 \\ -I_2^T \Omega & 0 & 0 & 0 & 0 \\ 0 & 0 & 0 & 0 & 0 \\ 0 & 0 & 0 & 2C_0\epsilon_1 & 0 \\ 0 & 0 & 0 & 0 & 2C_0\epsilon_1 \end{vmatrix}; \quad (3.53)$$

$$\bar{K} = \begin{vmatrix} 0 & 0 & 0 & 0 & 0 \\ 0 & 0 & 0 & 0 & 0 \\ 0 & 0 & 0 & 0 & 0 \\ 0 & 0 & 0 & \epsilon_1^2 & 0 \\ 0 & 0 & 0 & 0 & \epsilon_2^2 \end{vmatrix}; \quad (3.54)$$

And if we assume control is applied in the Θ_2 direction only, without any action to the flexible appendages, we have:

$$\bar{B} = \begin{vmatrix} \bar{B}_R \\ \bar{B}_E \end{vmatrix} = \begin{vmatrix} 0 \\ 0 \\ b_1 \\ 0 \\ 0 \end{vmatrix}; \quad (3.55)$$

By choosing a state vector x as shown below

$$x = [r^T, \dot{r}^T]^T; \quad (3.56)$$

The equation of motion can be placed in the form

$$\dot{x} = Fx + Gu; \quad (3.57)$$

where

$$F = \begin{vmatrix} 0 & I \\ -\bar{m}^{-1}\bar{K} & -\bar{m}^{-1}\bar{D} \end{vmatrix}; \quad (3.58)$$

and

$$G = \begin{vmatrix} 0 \\ \bar{m}^{-1}\bar{B} \end{vmatrix}; \quad (3.59)$$

where 0 and I are null and identity matrices resp.

3.3 Evaluation Model

A work model is used in the synthesis and the implementation of control. An evaluation model represents the physical system for simulations and analyses. It is extended to include an observation scheme and account for dynamic noise.

If dynamic noise is to be considered, the equation of motion in state variable form (equation 3.57) can be extended to:

$$\dot{x} = Fx + Gu + L\omega \quad ; \quad (3.60)$$

where ω is a gaussian noise with

$$E(\omega) = 0 \quad ; \quad (3.61)$$

$$E(\omega \cdot \omega^T) = Q \quad ; \quad (3.62)$$

For the idealized spacecraft, we assume $L = G$; (3.63). The observations can be obtained by,

$$y = Hx + v \quad ; \quad (3.64)$$

where H is the observation matrix and v is a noise vector with zero mean, having a covariance matrix equal to R .

$$E(v \cdot v^T) = R \quad ; \quad (3.65)$$

For the idealized spacecraft, we observe the variable Θ_z only. Therefore, the observations can be obtained by,

$$y = h_1 \Theta_z + v \quad ; \quad (3.66)$$

where h_1 can be simply considered as a scaling factor.

3.3 (Cont'd)

Having defined the state-space system, the numerical parameters remain to be chosen. Typical parameter values for a spacecraft similar to the Hughes HS 393 with Harris-like antenna reflectors are listed as follows:

- a) 2100 Kg for the global weight
- b) 1400 Kg for the rotor weight
- c) Rigid body with a 3.6 meter diameter, 10 meter height, 50 Kg reflector mass and a spinning body rotation frequency of .75 Hz.
- d) 5 meter beam equivalent length for the reflector
- e) First modal frequencies of .35 and .50 Hz.
- f) Damping coefficient set to .005.

The values of h_1 and b_1 are chosen to be 100, 1 respectively. Q is assumed to have a typical value of 10^{-4} and R is assumed an initial value of 10^{-6} . All assumed parameters were each varied to provide an idea of how the variation affected the end results (sensitivity observations). All estimated or assumed parameters are tabulated in Tables 3-1 to 3-3.

3.4 Control of Despun Platform

The problem considered in this section is the control of the despun platform about the spin axis. For this application, one possible solution involves the use of a second order work model.

Using equations 3.58, 3.59 and 3.63, the second order work model can be given by

$$F_1 = \begin{vmatrix} 0 & 1 \\ 0 & 0 \end{vmatrix} ; (3.67)$$

$$L_2 = G_2 = \begin{vmatrix} 0 \\ b_1/J_z \end{vmatrix} ; (3.68)$$

$$y = h_1 \theta_z + v ; (3.69)$$

$$E(v \cdot v^T) = R ; (3.70)$$

$$E(\omega \cdot \omega^T) = Q ; (3.71)$$

3.4 (Cont'd)

If a regulator with constant gain is used, the control is given by,

$$u = C \hat{x} ; \quad (3.72)$$

where $\hat{x} = E(\bar{x}) ; \quad (3.73)$

$$\bar{x} = [\dot{\theta}_z, \ddot{\theta}_z]^T ; \quad (3.74)$$

The gain C is calculated considering the assumption that the following performance index is minimized.

$$J = \int_0^\infty (\bar{x}^T A \bar{x} + u^T B u) dt ; \quad (3.75)$$

We assume the following

- a) (F, G) controllable
- b) A is semi-definite positive
- c) R is definite positive
- d) (F, \sqrt{A}) is observable

If a filter with constant gain is used, a state estimate is given by,

$$\hat{x}_{k+1} = \bar{x}_{k+1} + K (y_{k+1} - \bar{H} \bar{x}_{k+1}) ; \quad (3.76)$$

where

$$\bar{x}_{k+1} = M \hat{x}_k + I u_k ; \quad (3.77)$$

$$I = \int_0^{T_s} m(T_s, y) g dy ; \quad (3.78)$$

TABLE 3-1 VALUES OF ESTIMATED PARAMETERS

TRIAL	1	2	3	4	5
J_x Kgm^2	8,000	8,000	8,000	8,000	8,000
$\cdot J_y$ Kgm^2	10,000	10,000	10,000	10,000	10,000
J_z Kgm^2	6,500	6,500	6,500	6,500	5,000
J_{xy}, J_{yx} Kgm^2	0	0	0	0	0
J_{xz}, J_{zx} Kgm^2	0	0	0	0	0
J_{zy}, J_{yz} Kgm^2	200	200	200	200	500
I_z^R Kgm^2	3,000	3,000	3,000	3,000	3,000
Q	10^{-4}	10^{-4}	10^{-4}	10^{-4}	10^{-4}
h_1	100	100	100	100	100
C_1	50	50	50	60	50
C_2	-50	-50	-50	-60	-50
b_1	1	1	1	1	1

TABLE 3-1 (cont'd)

TRIAL	1	2	3	4	5
C_a	.005	.005	.005	.005	.005
ω (Hz)	.75	.75	.75	.75	.57
σ_1 (Hz)	.35	.35	.15	.35	.35
σ_2 (Hz)	.50	.50	.20	.50	.50
R	10^{-6}	10^{-4}	10^{-6}	10^{-6}	10^{-6}

3.4 (Cont'd)

Where \bar{x}_k is the state coordinate in time t_k , M is a state transition matrix; T_s is the sampling period.

The gain K is calculated the Kalman filter for the processing of N observations.

The work model may have parameters which are similar to the evaluation model. Identical parameters are chosen for the idealized spacecraft model. The control gain is obtained setting $B_{11} = 1$ without loss of generality. The elements of matrix A should be chosen to conform to the critical spacecraft requirements of the despun section. For the idealized model, matrix A is chosen to be a diagonal matrix and two sets of values for A and control gain C are tabulated in Table 3-2.

TABLE 3-2

TRIALS	A11	A22	C1	C2
1	.100E+7	.100E+7	-.100E+4	-.374E+04
2	.100E+5	.100E+5	-.100E+3	-.114E+04

3.4 (Cont'd)

The values of M and I matrices found in equation 3.77 are functions of the control gain K, the dynamical parameters F and G and the sampling period Ts. Three different sets of filter gains are used for the idealized model:

- a) $T_s = .1$ with two options for control parameters (Trial 1 & 2 of table 3-3).
- b) $T_s = .4$ with the first set of control parameters (as in Trial 1) found in Trial 3 of Table 3-3.

Table 3-3 tabulates all values used (K, M, I) in the synthesis of the idealized model.

TABLE 3-3

TRIAL	1	2	3
T _s	0.1	0.1	0.4
Control Trial	1	2	1
K ₁	.306E-02	.334E-02	.185E-02
K ₂	.370E-02	.491E-02	.270E-04
M ₁₁	1.	1.	1.
M ₁₂	0.1	0.1	0.4
M ₂₁	0.	0.	0.
M ₂₂	1.	1.	1.
I ₁₁	.770E-06	.770E-06	.123E-04
I ₂₁	.154E-04	.154E-04	.616E-04

3.5 SIMULATION RESULTS

The plots of the simulation results are included in Appendix A. The following plots are included for various trials:

- a) $\dot{\theta}_z$ - Angular Drift
- b) $\ddot{\theta}_z$ - Angular Velocity
- c) $\dot{\theta}_x$ - Angular Velocity
- d) $\dot{\theta}_y$ - Angular Velocity
- e) q_1 - Generalized coordinate
- f) q_2 - Generalized coordinate

all as a function of time.

The initial conditions were chosen as 5 mrad for $\dot{\theta}_z$ angular drift of the despun section and 1 mrad/sec for the angular velocities $\dot{\theta}_y, \dot{\theta}_x$.

The results were obtained using values from Tables 3-1, 3-2 and 3-3. The figures are classified by the notation Trial = i, j, k. The first, second and third subscripts (i, j, k) correspond to trial i from Table 3-1, Trial j from Table 3-2 and Trial k from Table 3-3.

Plots were obtained for trials 1-1-1, 2-1-1, 3-1-1, 4-1-1, 5-1-1, 1-2-2 and trial 1-1-3.

The trials were chosen to illustrate the sensitivity of the system. Trial 2-1-1 serves to illustrate the influence of noisy environments through the controller.

A control scheme could be chosen to minimize this effect.

Trial 4-1-1 was chosen to illustrate system sensitivity as functions of parameters c_1 and c_2 (See Eqn. 3.48, 3.49). The system was found to be unstable when c_1, c_2 were increased by 20%. The designed system must be robust for this degree of variation due to the restricted fidelity modelling of a complex spacecraft.

4. CONCLUSIONS

This work fulfills the objective of presenting a generalized dynamical model for a spin stabilized elastic spacecraft. The model is applied to simulate a simple idealized spacecraft. The results show the potential of having a destabilizing influence on the controlled system due to appendage flexibility.

The attitude control of the elastic spacecraft is a critical problem. 'Robustness' is illustrated to be an important control system requirement due to truncated coordinate in the work model with even more robustness required due to restricted fidelity in modelling of the evaluation model.

An analysis using simulation and numerical techniques for determining parameter variation sensitivity and stability analysis must be realized. Some basic technical resources are necessary to permit the qualification and/or design of an M-SAT-like spacecraft.

Some requirements are discussed as follows:

The generalized dynamic model presented in this work can be used for an M-SAT-like spacecraft. To obtain the numerical parameters requires the use of an eigenvalue/eigenvector program, a finite element program such as NASTRAN and complete information about the physical characteristics of the spacecraft.

The synthesis of the control system should serve to define important features of an M-SAT-like spacecraft such as simplicity and reliability and provide design flexibility and adaptability to new missions. The elastic spacecraft control laws used do not alone necessarily serve to establish a better solution but studies of the current technical development in this area are also very important for this problem.

The dynamic analysis of flexible spacecraft involves the use of established procedures. Numerical simulation is a good tool but does not provide information about parameter sensitivity as the results can be dependent on initial conditions, however, numerical simulation used in conjunction with classical root-locus and eigenvalue analysis should provide an efficient procedure for this problem.

5. APPENDIX A

SIMULATION PLOTS

FIG A. 1-1 θ_z -ANGULAR DRIFT
GRAPH FOR VALUES CORRESPONDING
TO TRIAL #1-1-1
— ANGULAR DRIFT (RAD.)

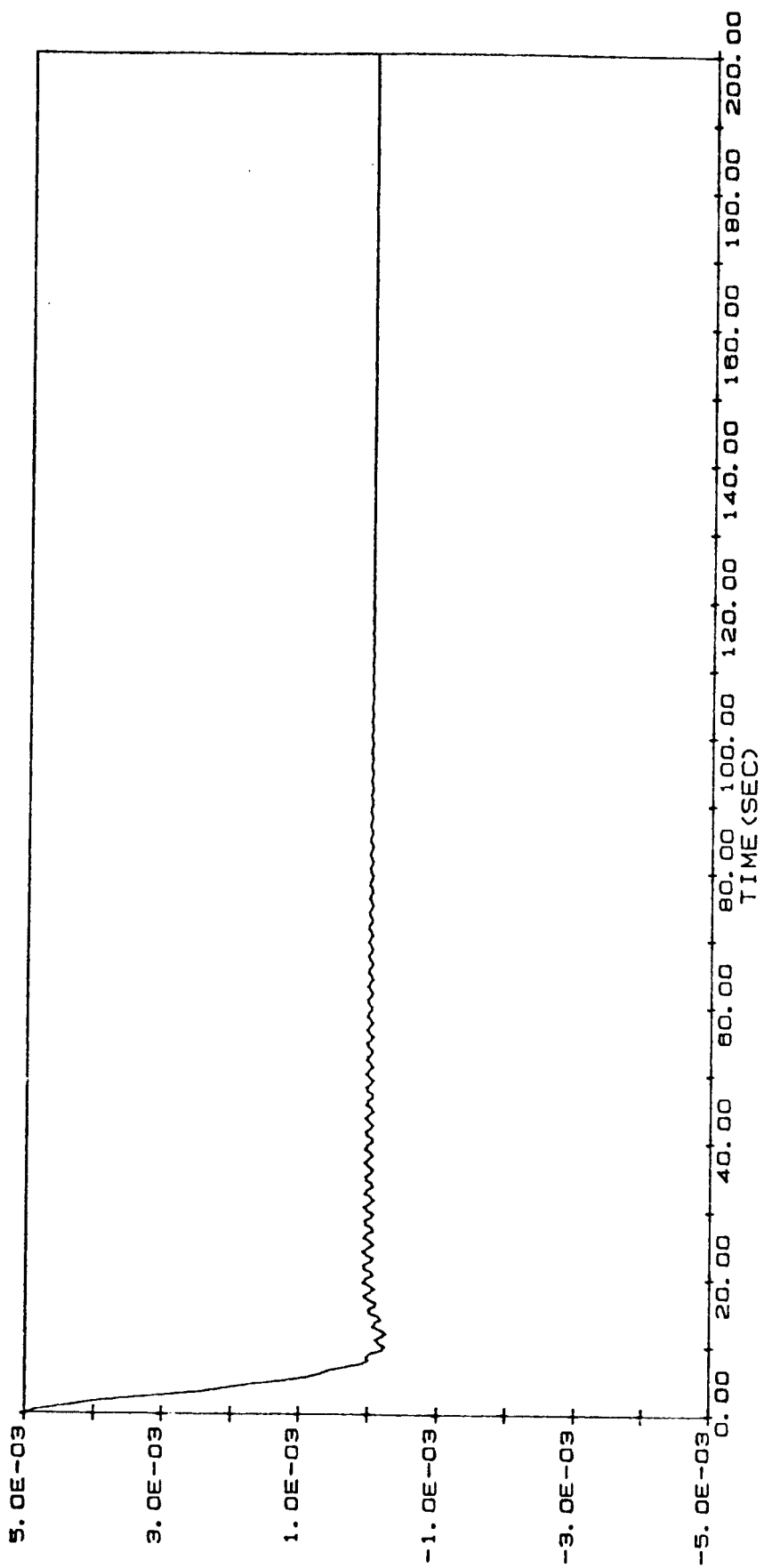


FIG A. 2-1 $\dot{\theta}_z$ -ANGULAR VELOCITY
GRAPH FOR VALUES CORRESPONDING
TO TRIAL #1-1-1
— ANGULAR VELOCITY (RAD/SEC)

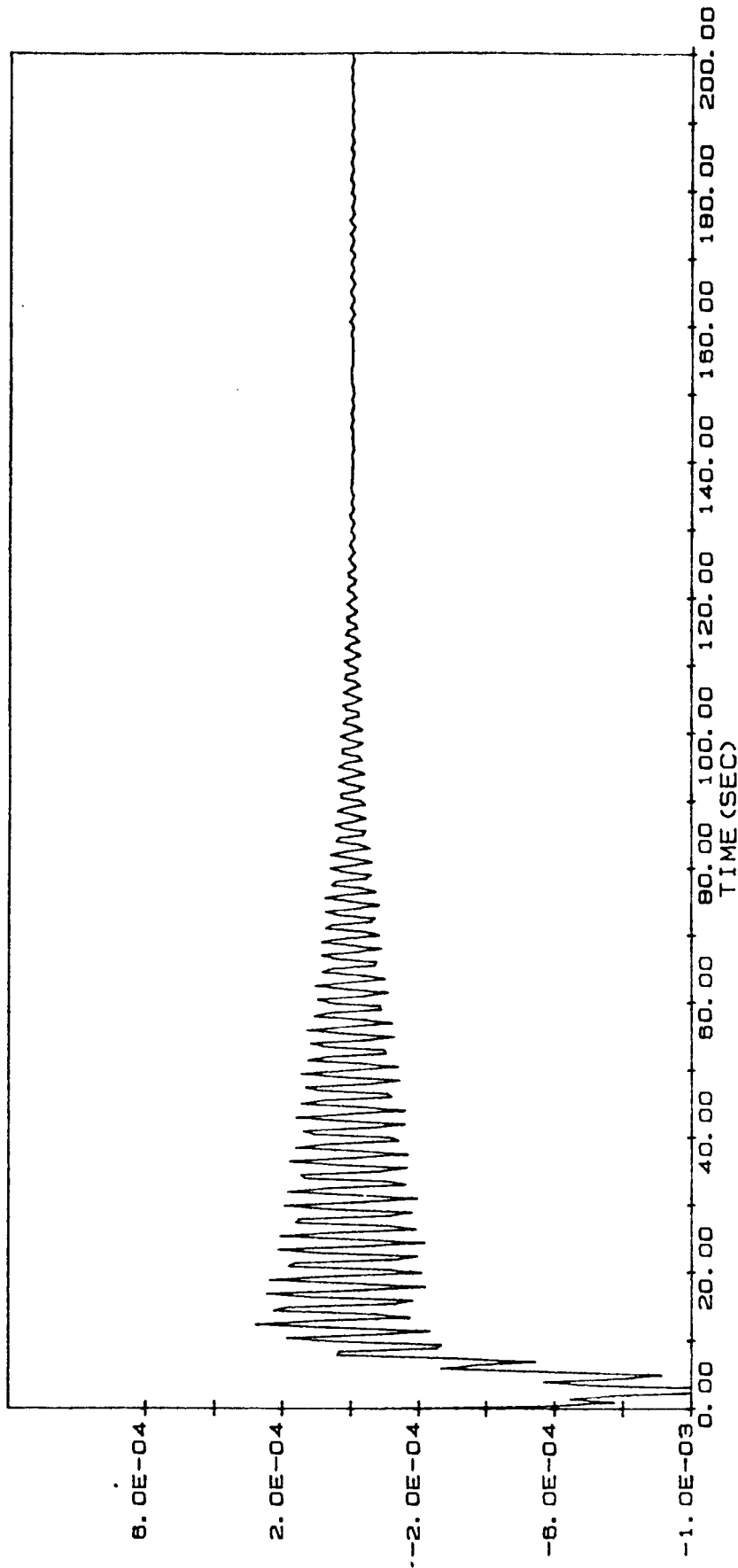


FIG A. 3-1 $\dot{\theta}_x$ -ANGULAR VELOCITY
GRAPH FOR VALUES CORRESPONDING
TO TRIAL #1-1-1
— ANGULAR VELOCITY (RAD/SEC)

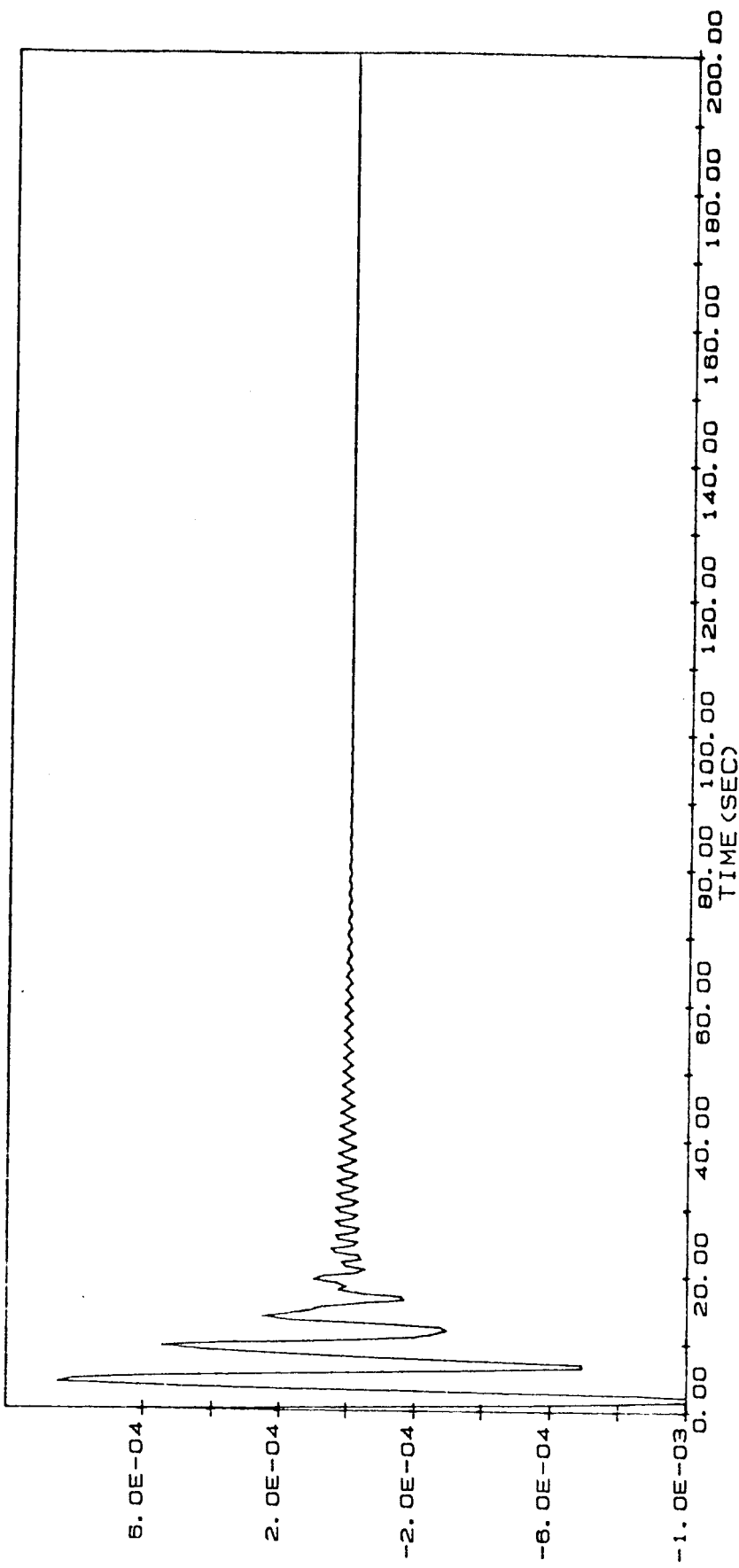


FIG A. 4-1 $\dot{\theta}_y$ -ANGULAR VELOCITY
GRAPH FOR VALUES CORRESPONDING
TO, TRIAL #1-1-1
— ANGULAR VELOCITY (RAD/SEC)

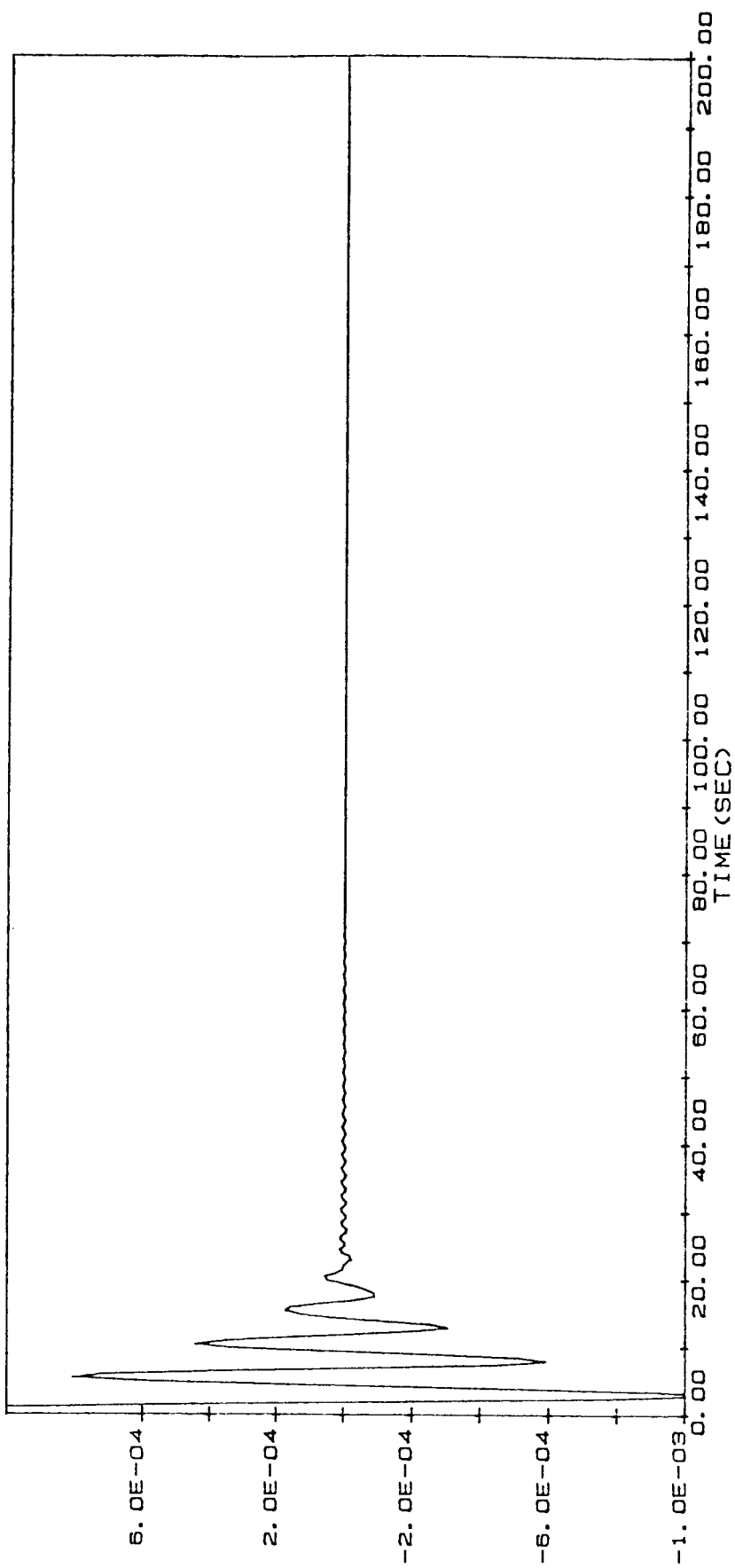


FIG A. 5-1 q₁-GEN. COORDINATE
GRAPH FOR VALUES CORRESPONDING
TO, TRIAL #1-1-1
GENERALIZED COORDINATE (q₁)

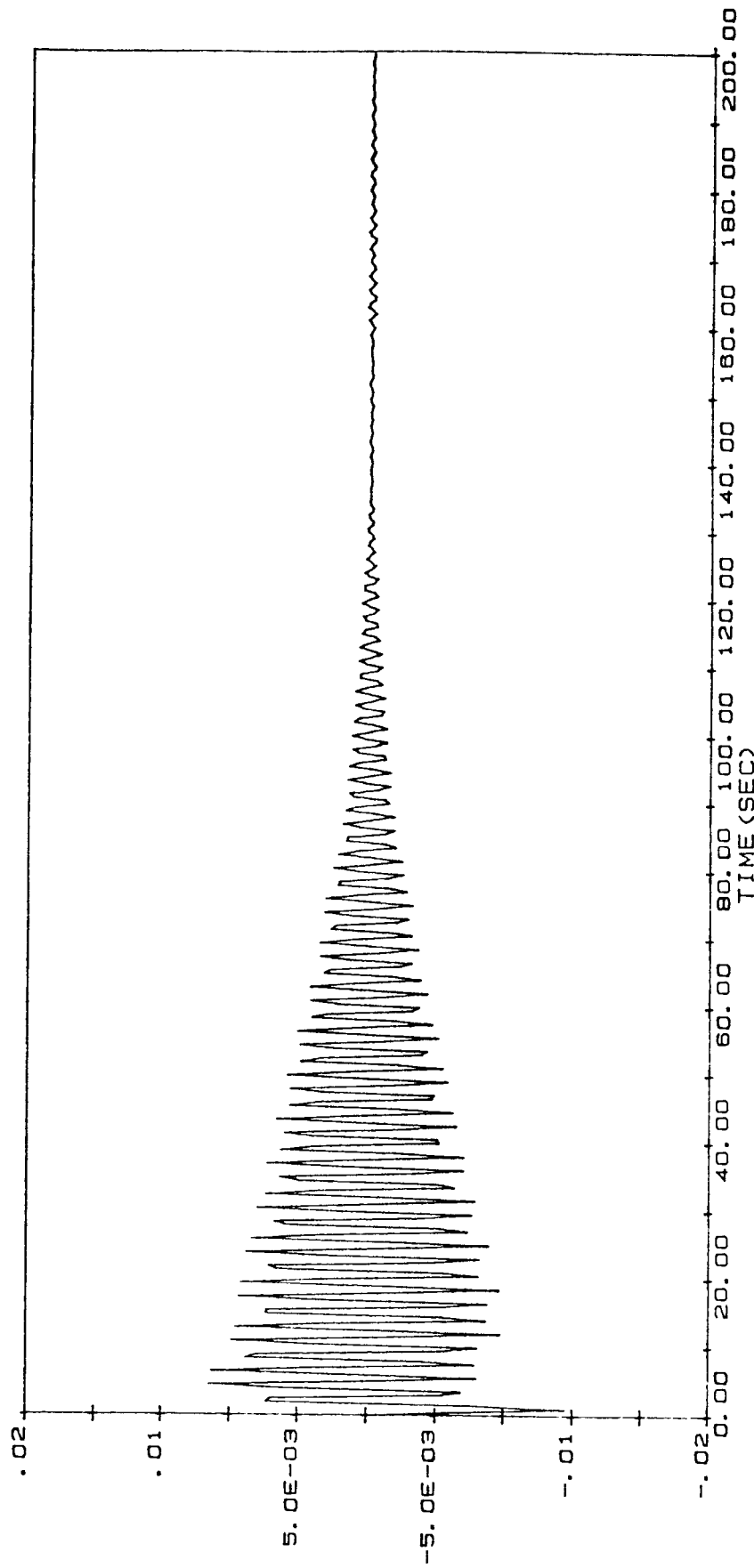


FIG A. 6-1 q2-GEN. COORDINATE
GRAPH FOR VALUES CORRESPONDING
TO TRIAL #1-1-1
GENERALIZED COORDINATE (q2)

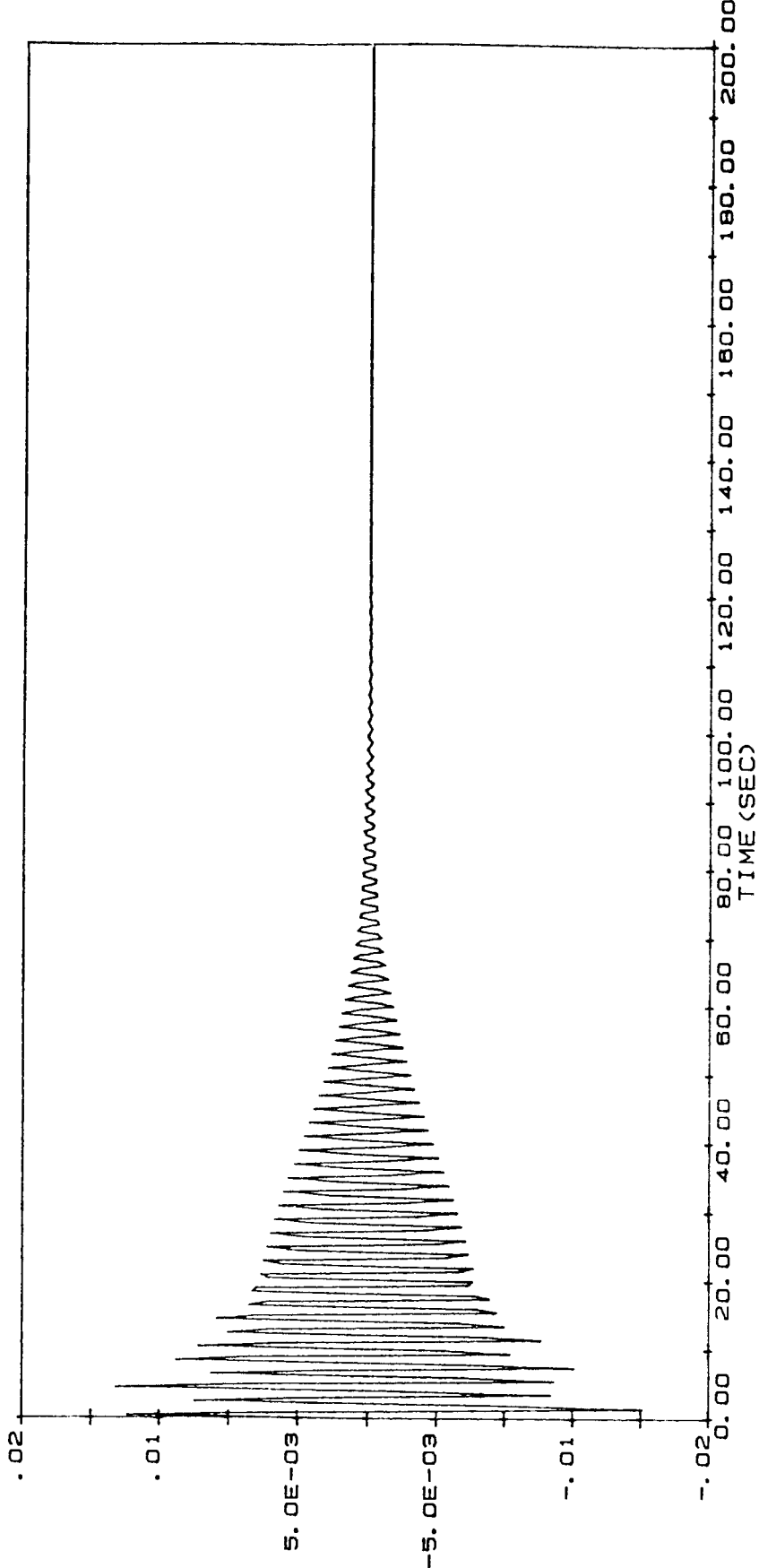


FIG A. 1-2 θ_z -ANGULAR DRIFT
GRAPH FOR VALUES CORRESPONDING
TO TRIAL #2-1-1
— ANGULAR DRIFT (RAD.)

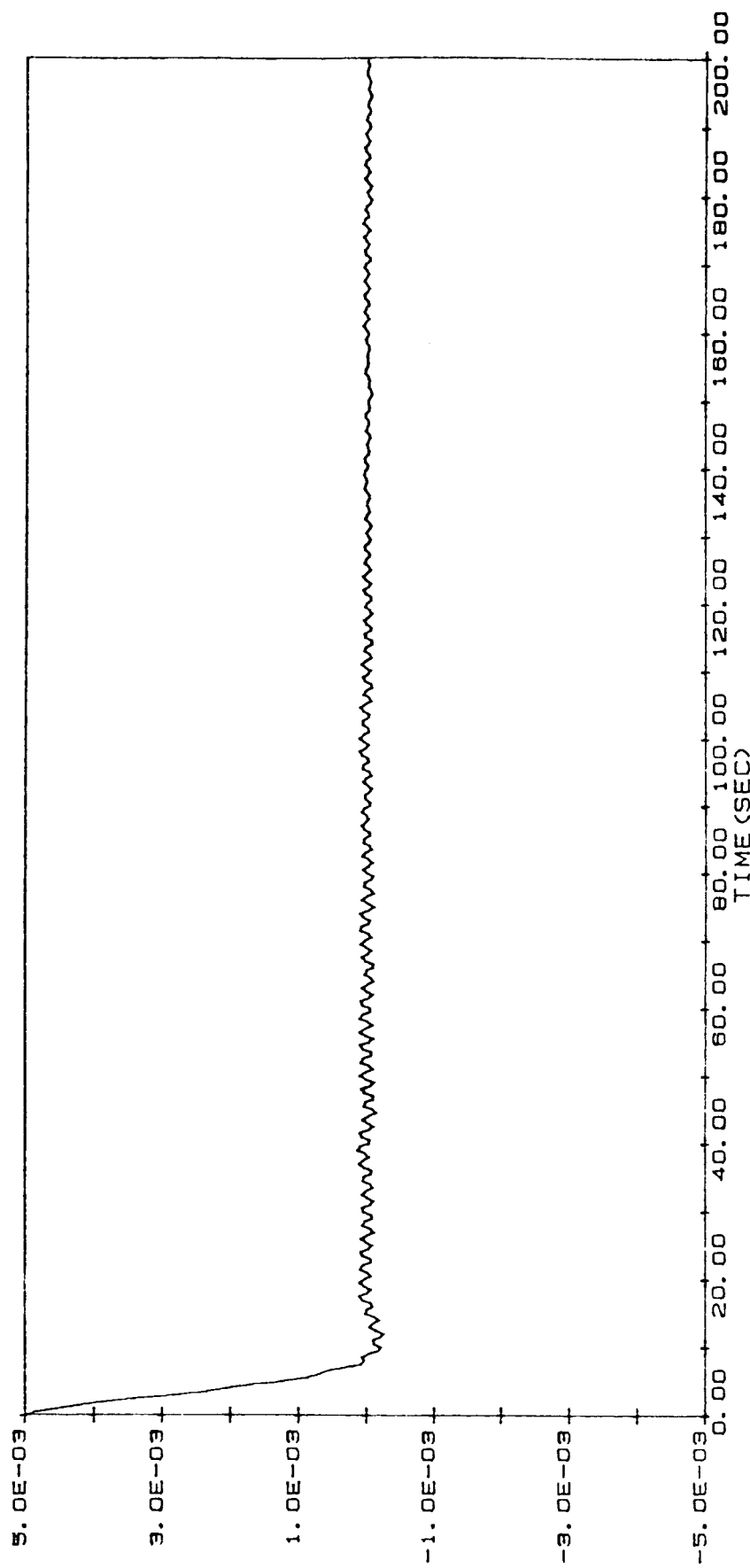


FIG A. 2-2 $\dot{\theta}_z$ -ANGULAR VELOCITY
GRAPH FOR VALUES CORRESPONDING
TO TRIAL #2-1-1
— ANGULAR VELOCITY (RAD/SEC)

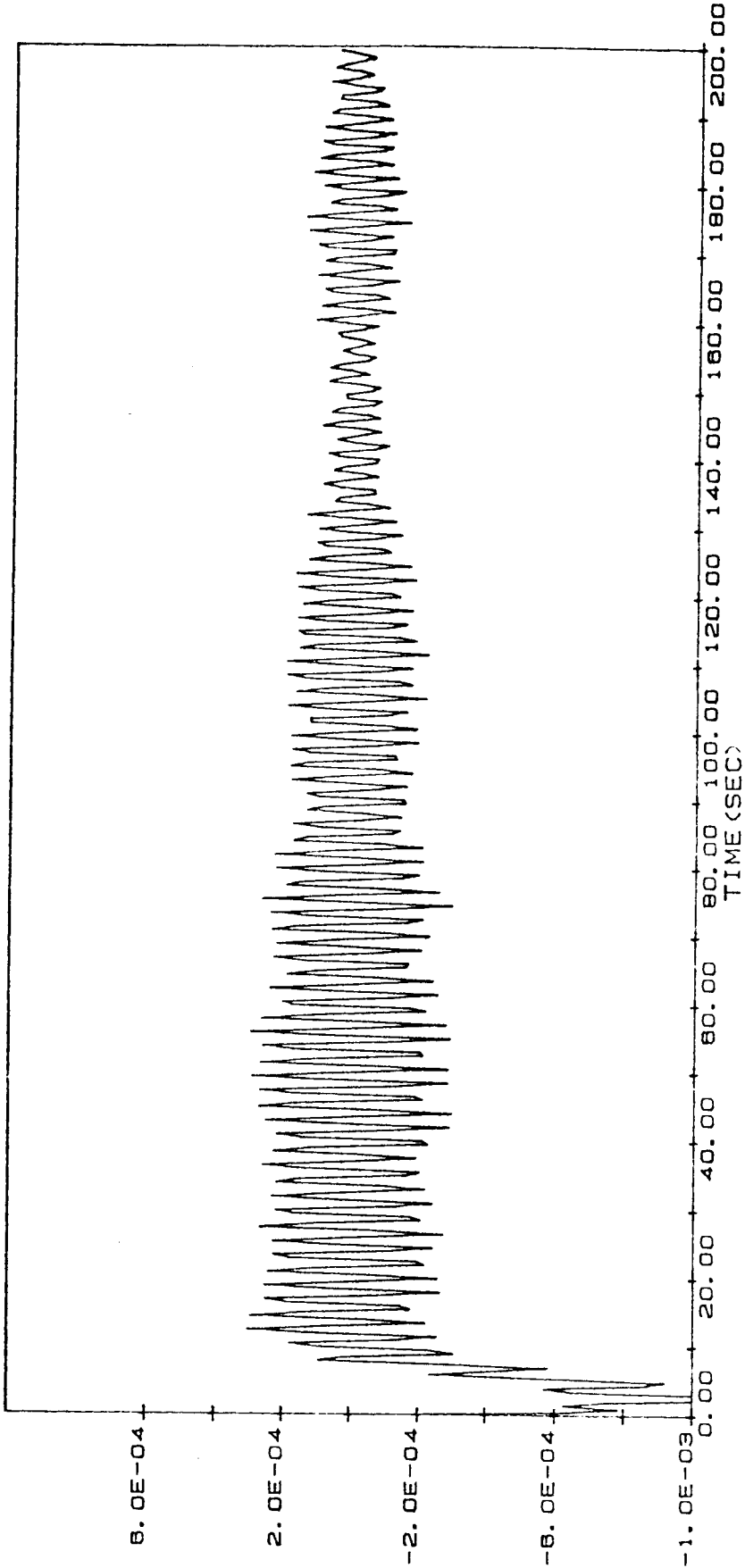


FIG A. 3-2 $\dot{\theta}_x$ -ANGULAR VELOCITY
GRAPH FOR VALUES CORRESPONDING
TO TRIAL #2-1-1
— ANGULAR VELOCITY (RAD/SEC)

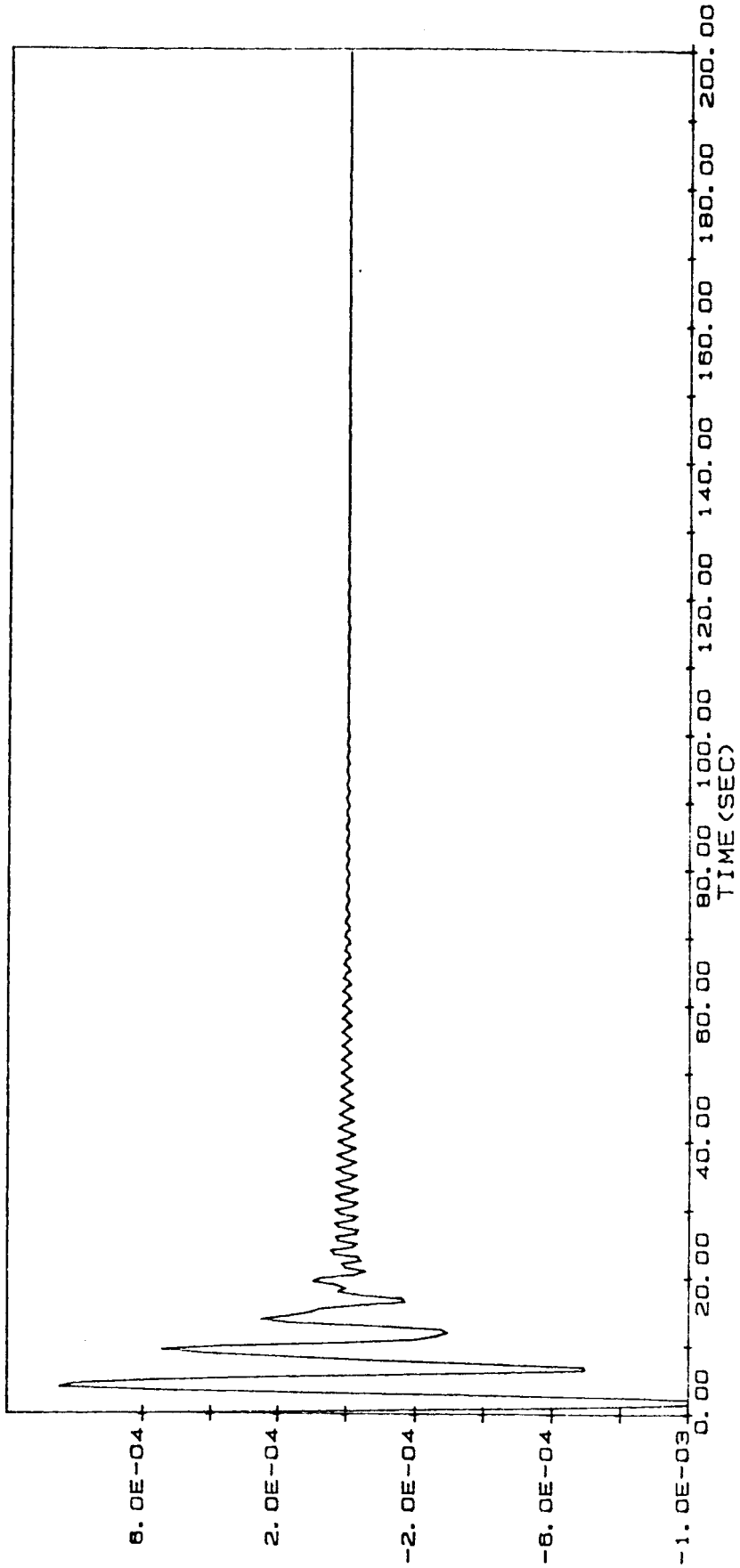


FIG A. 4-2 $\dot{\theta}_y$ -ANGULAR VELOCITY
GRAPH FOR VALUES CORRESPONDING
TO TRIAL #2-1-1
— ANGULAR VELOCITY (RAD/SEC)

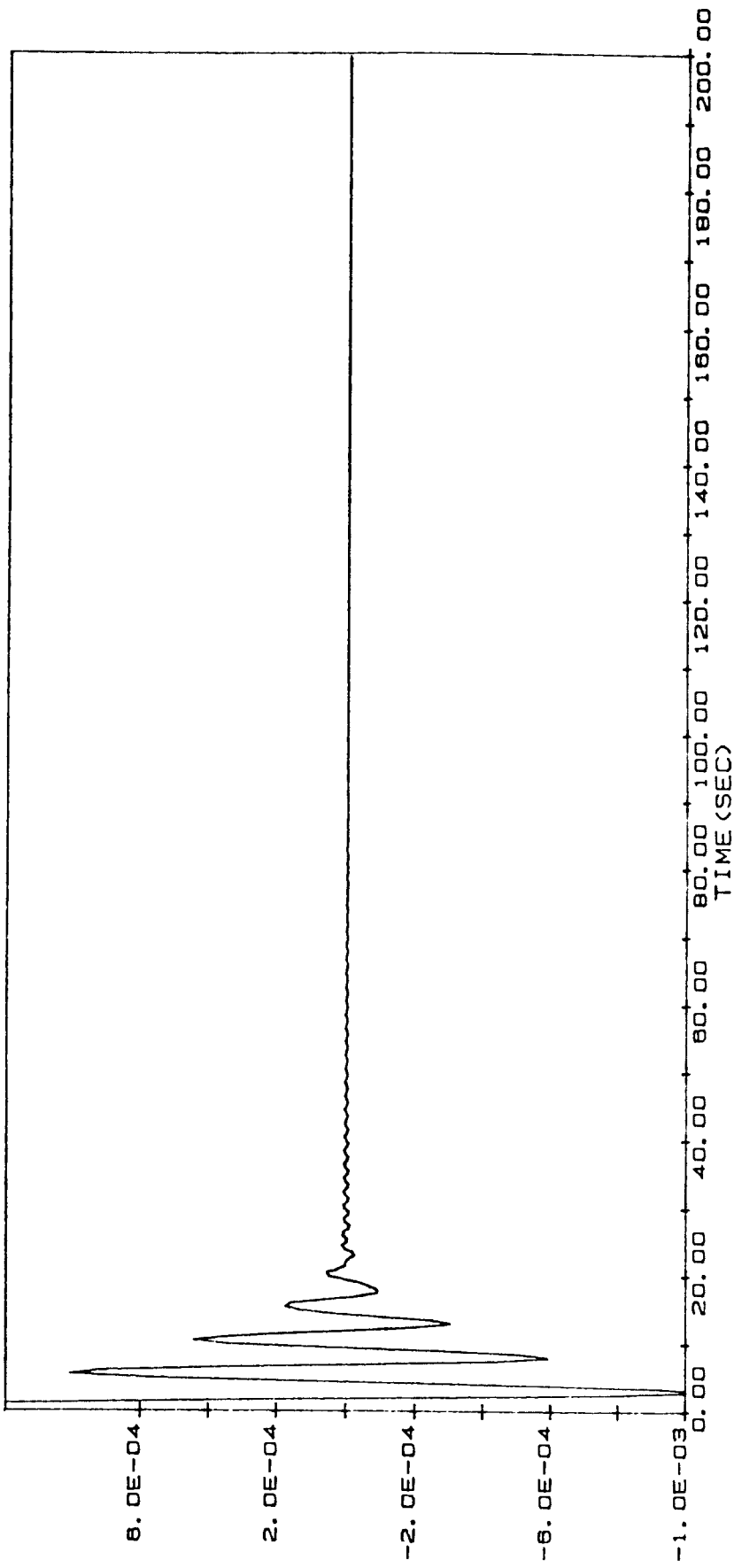


FIG A. 5-2 q₁-GEN. COORDINATE
GRAPH FOR VALUES CORRESPONDING
TO TRIAL #2-1-1
— GENERALIZED COORDINATE (q₁)

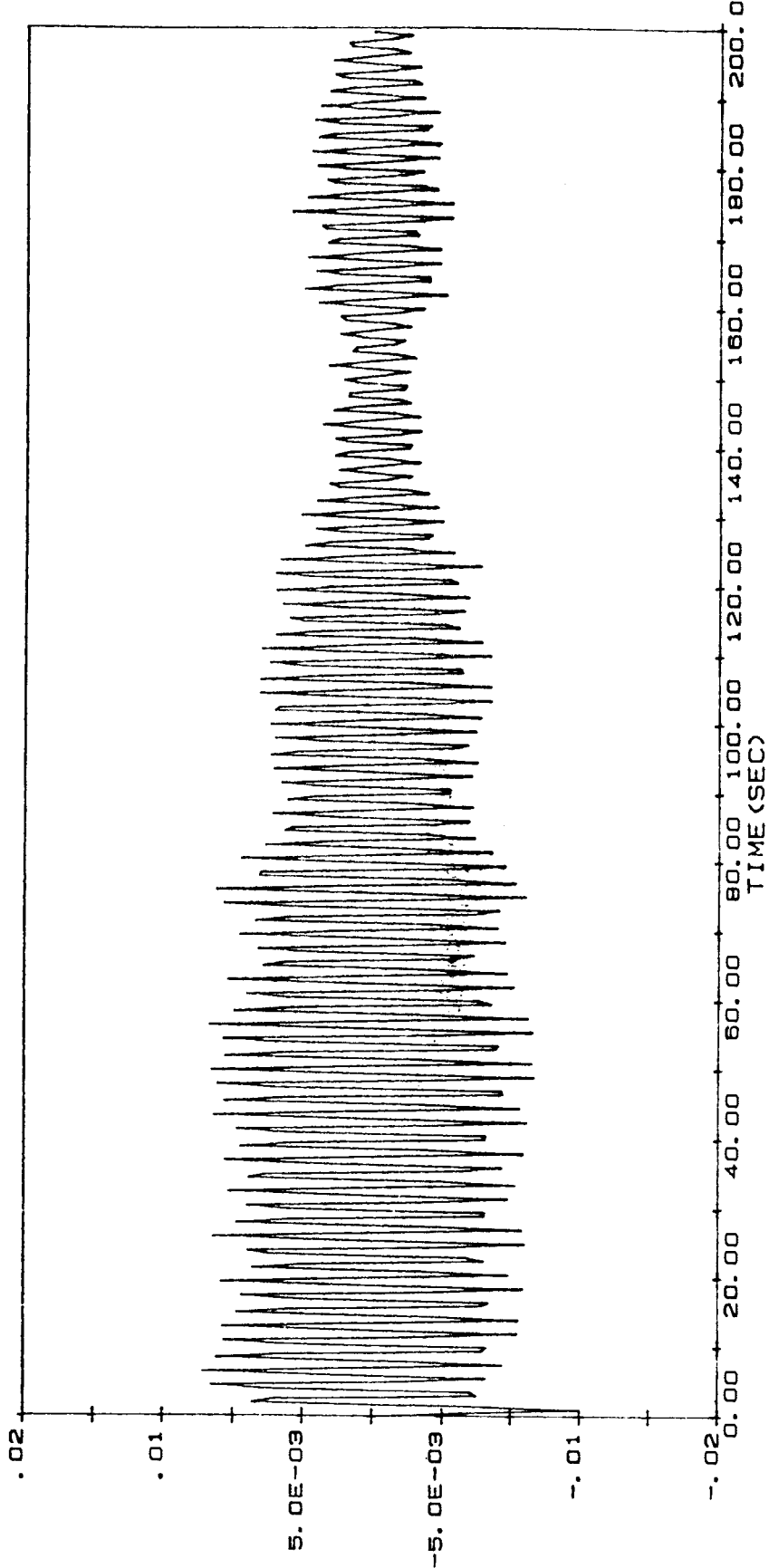


FIG A. 6-2 q2-GEN. COORDINATE
GRAPH FOR VALUES CORRESPONDING
TO TRIAL #2-1-1
GENERALIZED COORDINATE (q2)

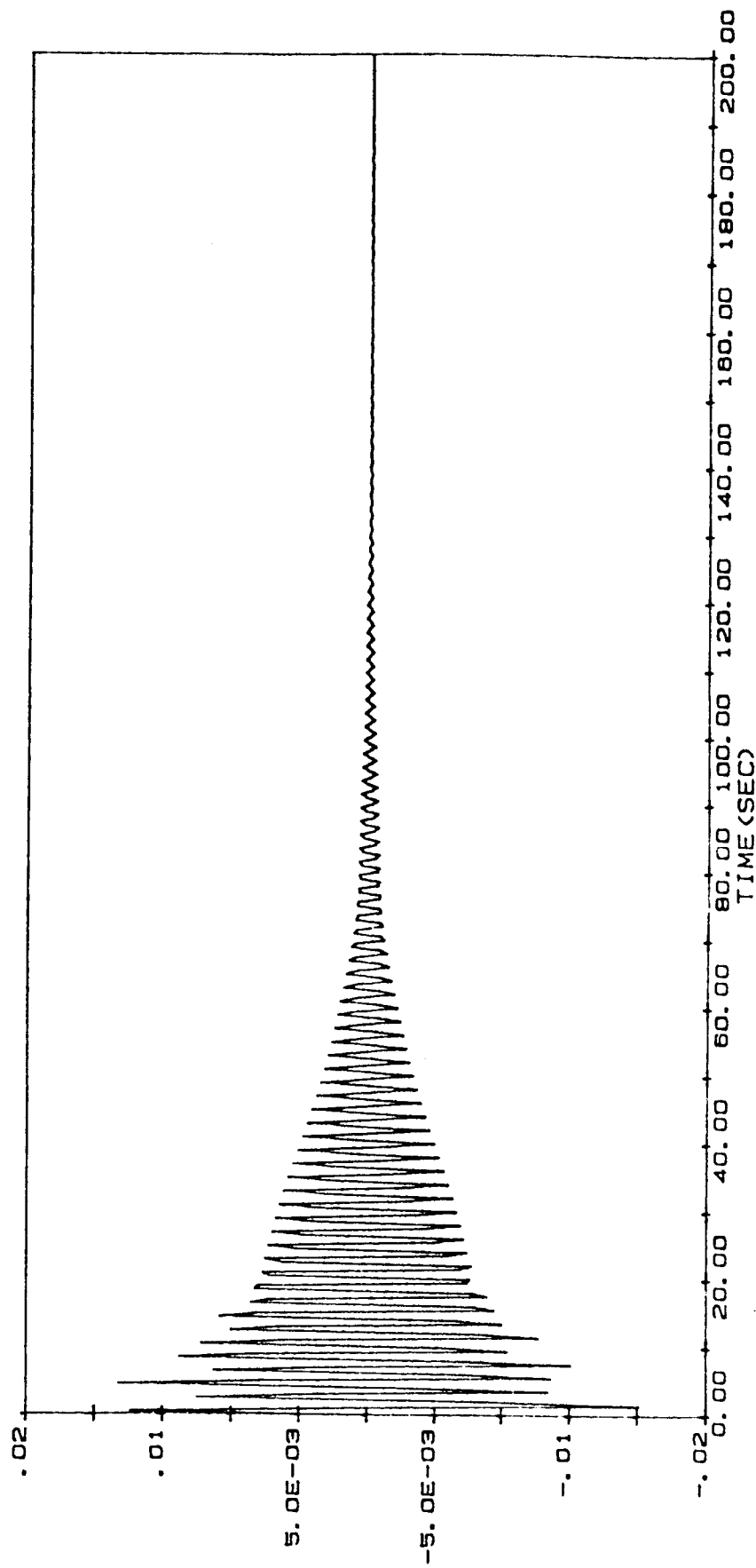


FIG A. 1-3 θ_z -ANGULAR DRIFT
GRAPH FOR VALUES CORRESPONDING
TO TRIAL #3-1-1
— ANGULAR DRIFT (RAD.)

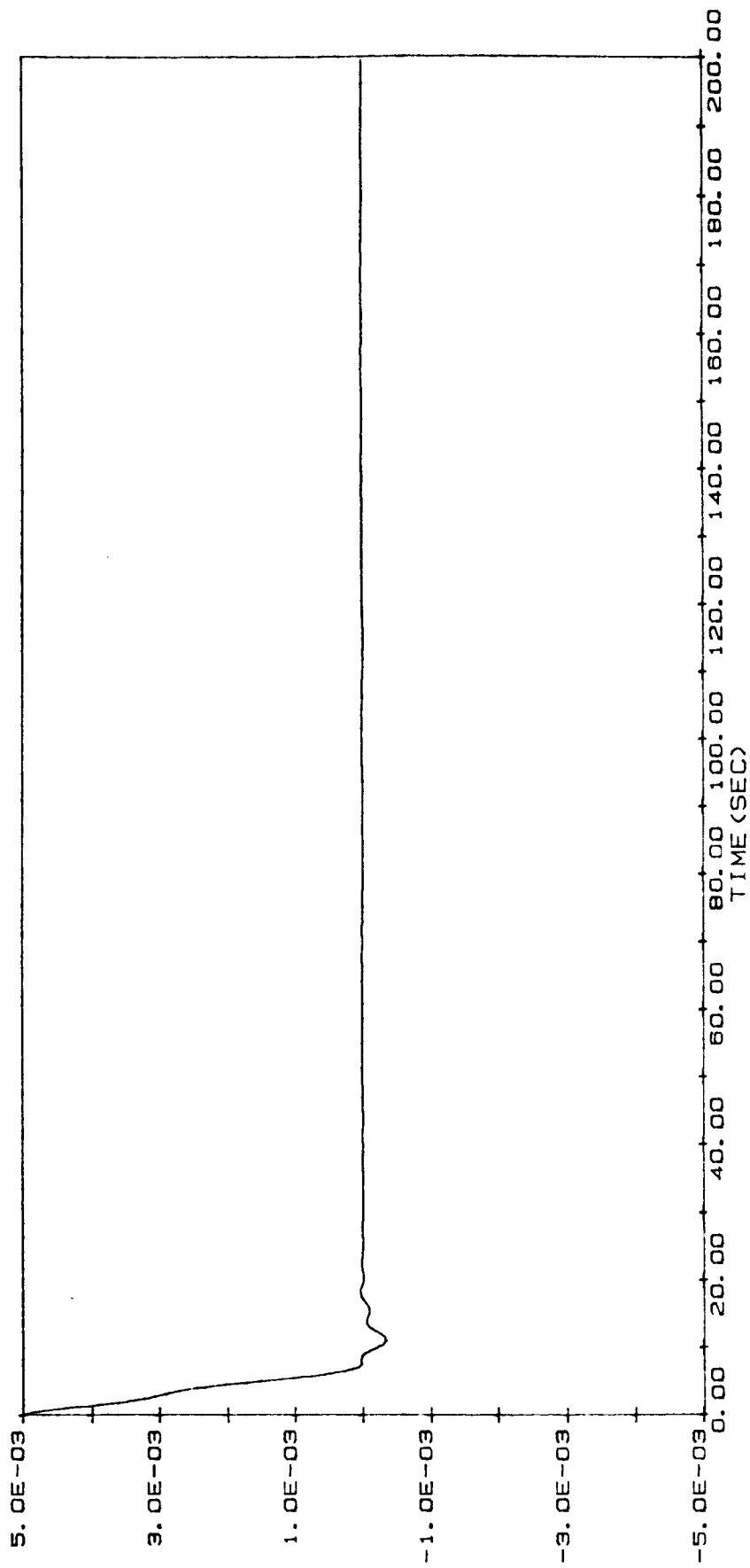


FIG A. 2-3 $\dot{\theta}_z$ -ANGULAR VELOCITY
GRAPH FOR VALUES CORRESPONDING
TO TRIAL #3-1-1
— ANGULAR VELOCITY (RAD/SEC)

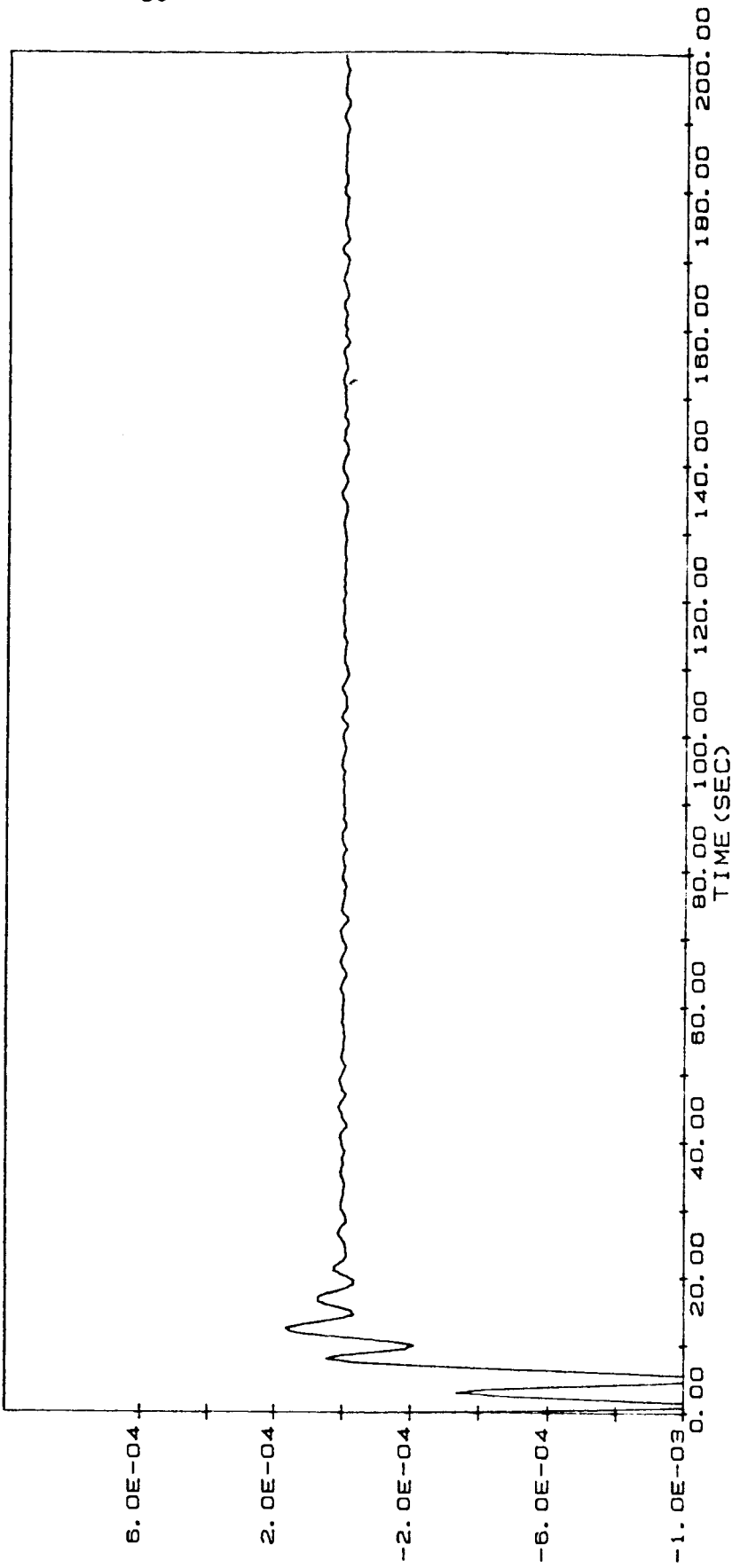


FIG A. 3-3 $\dot{\theta}_x$ -ANGULAR VELOCITY
GRAPH FOR VALUES CORRESPONDING
TO TRIAL #3-1-1
— ANGULAR VELOCITY (RAD/SEC)

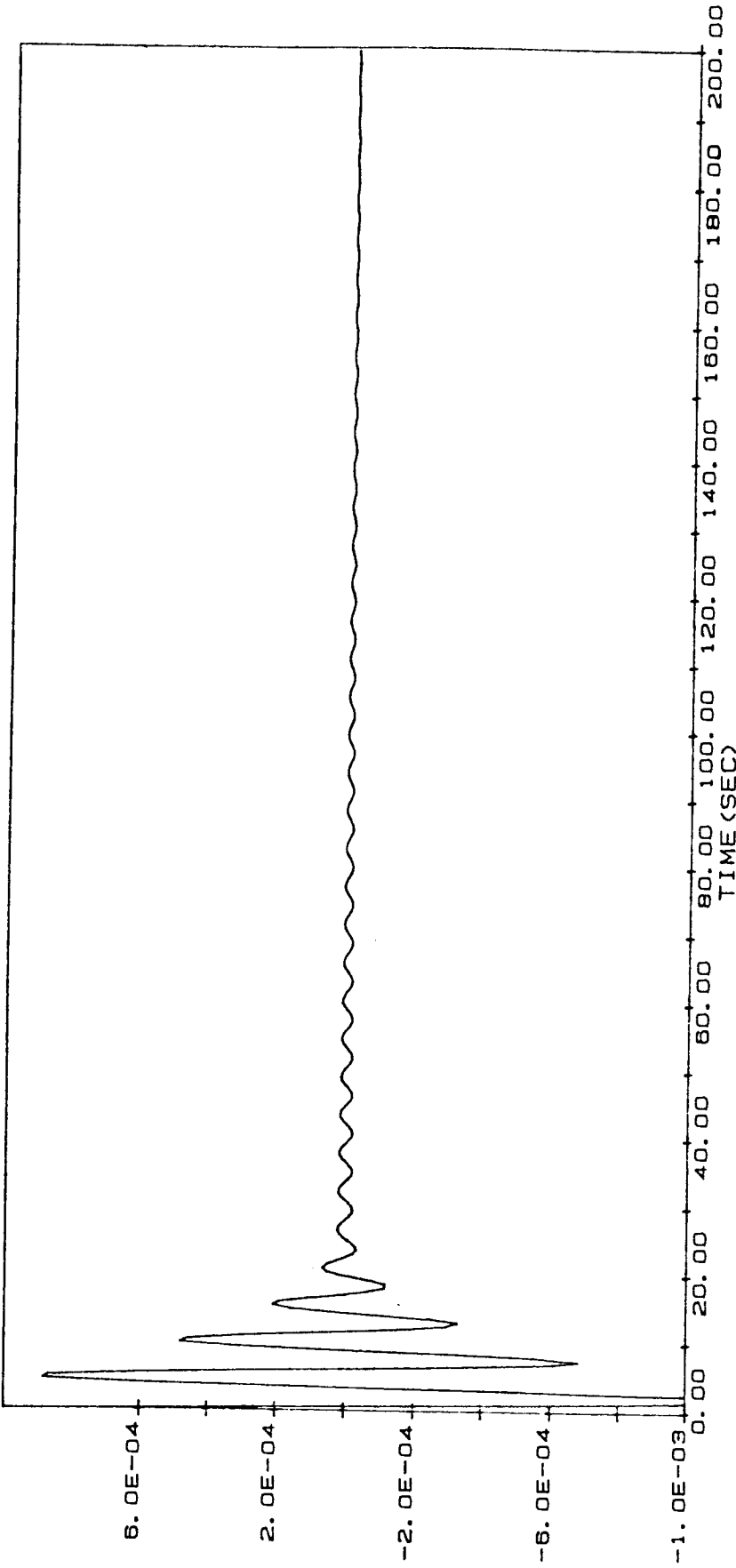


FIG A. 4-3 $\dot{\theta}_y$ -ANGULAR VELOCITY
GRAPH FOR VALUES CORRESPONDING
TO TRIAL #3-1-1
— ANGULAR VELOCITY (RAD/SEC)

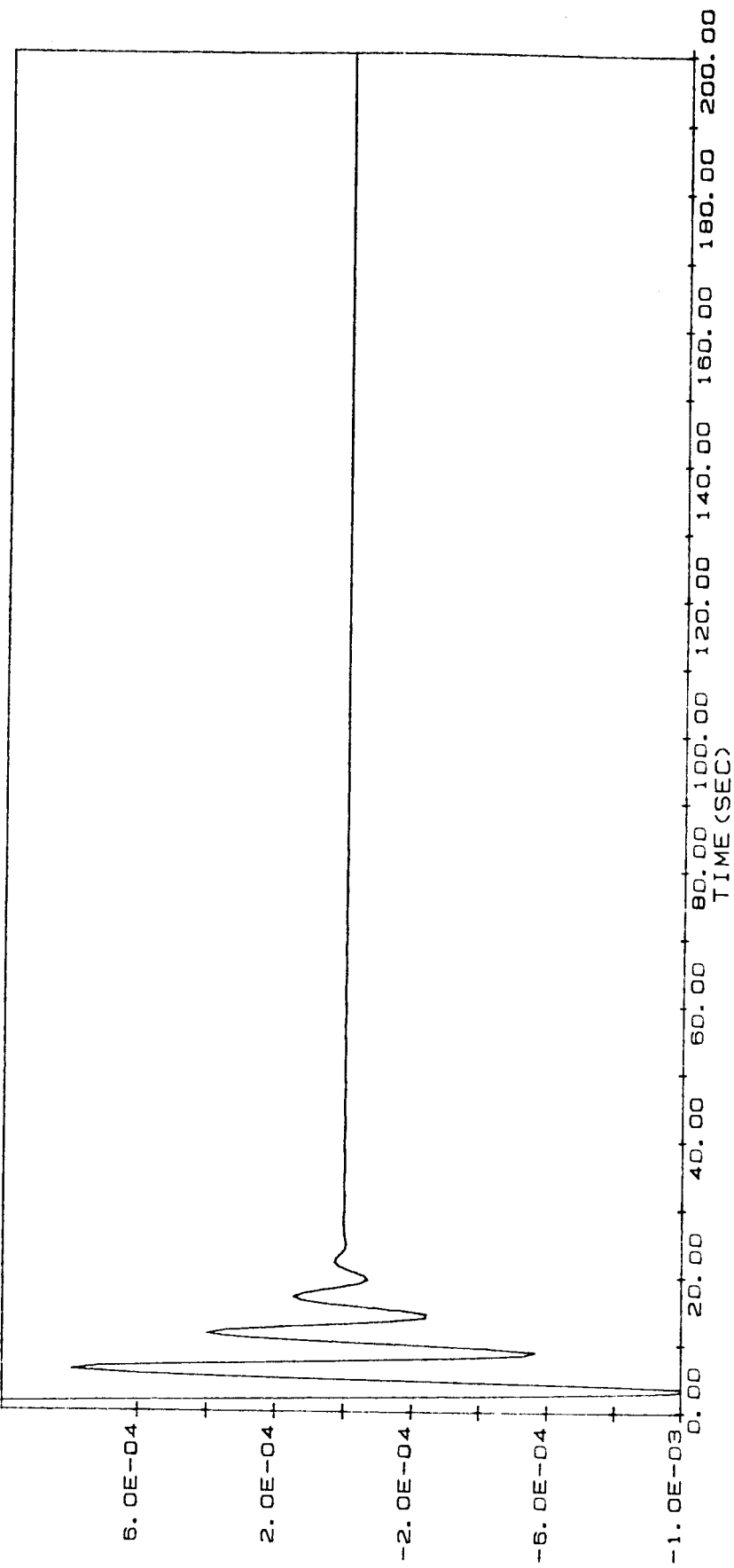


FIG A. 5-3 q1-CEN. COORDINATE
GRAPH FOR VALUES CORRESPONDING
TO TRIAL #3-1-1
— GENERALIZED COORDINATE (q1)

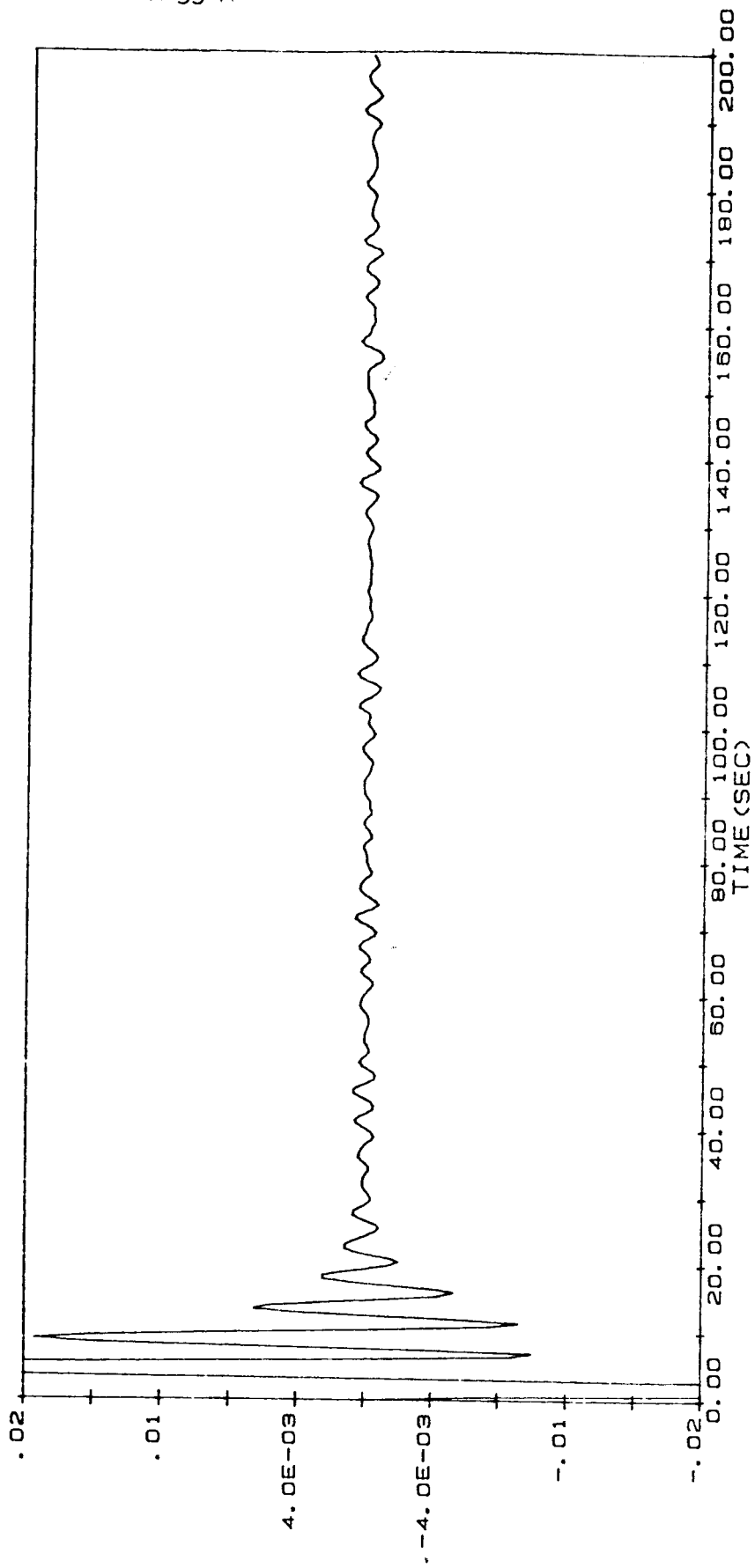


FIG A. 6-3 q2-CEN. COORDINATE
GRAPH FOR VALUES CORRESPONDING
TO, TRIAL #3-1-1
GENERALIZED COORDINATE (q2)

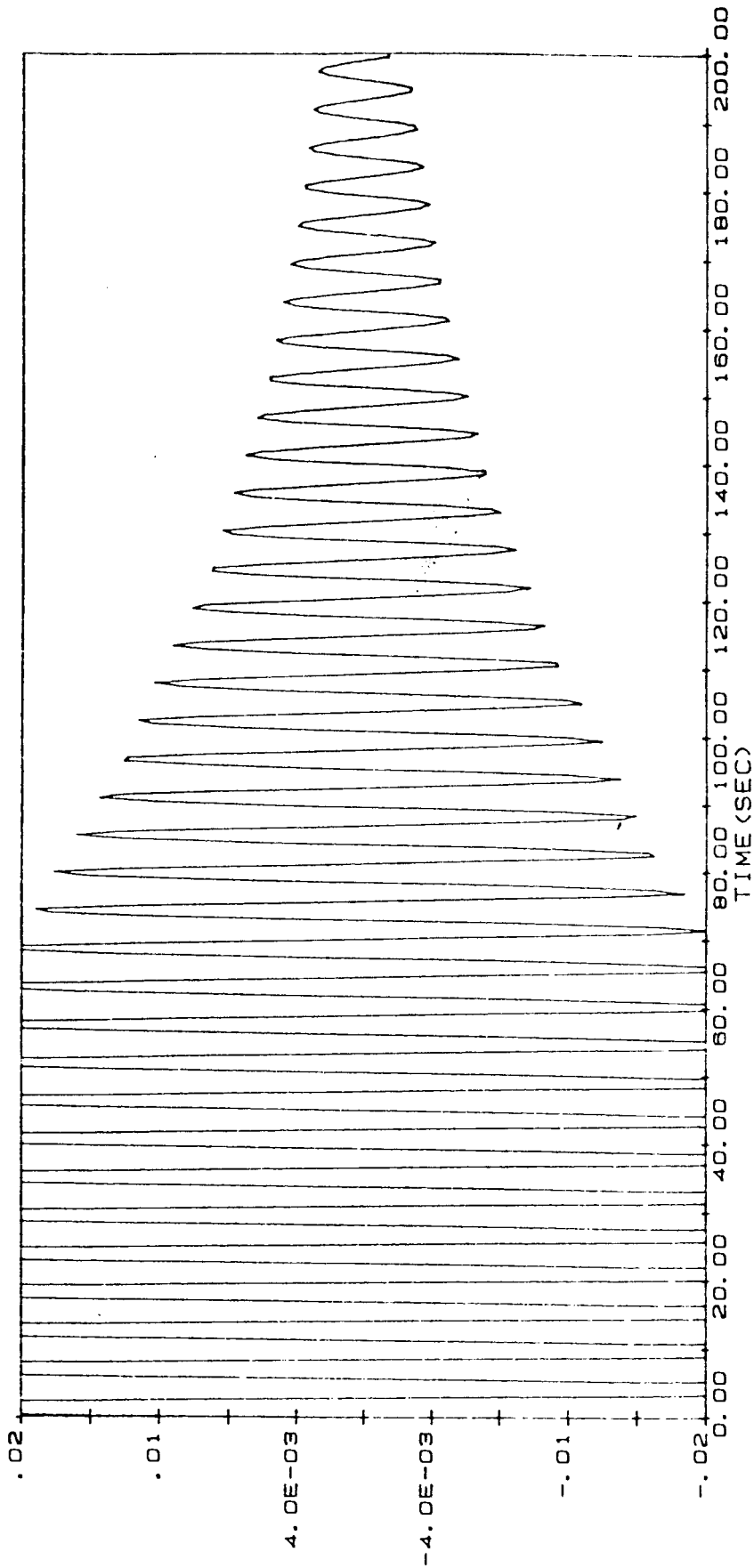


FIG A. 1-4 θ_z -ANGULAR DRIFT
GRAPH FOR VALUES CORRESPONDING
TO TRIAL #4-1-1
— ANGULAR DRIFT (RAD.)

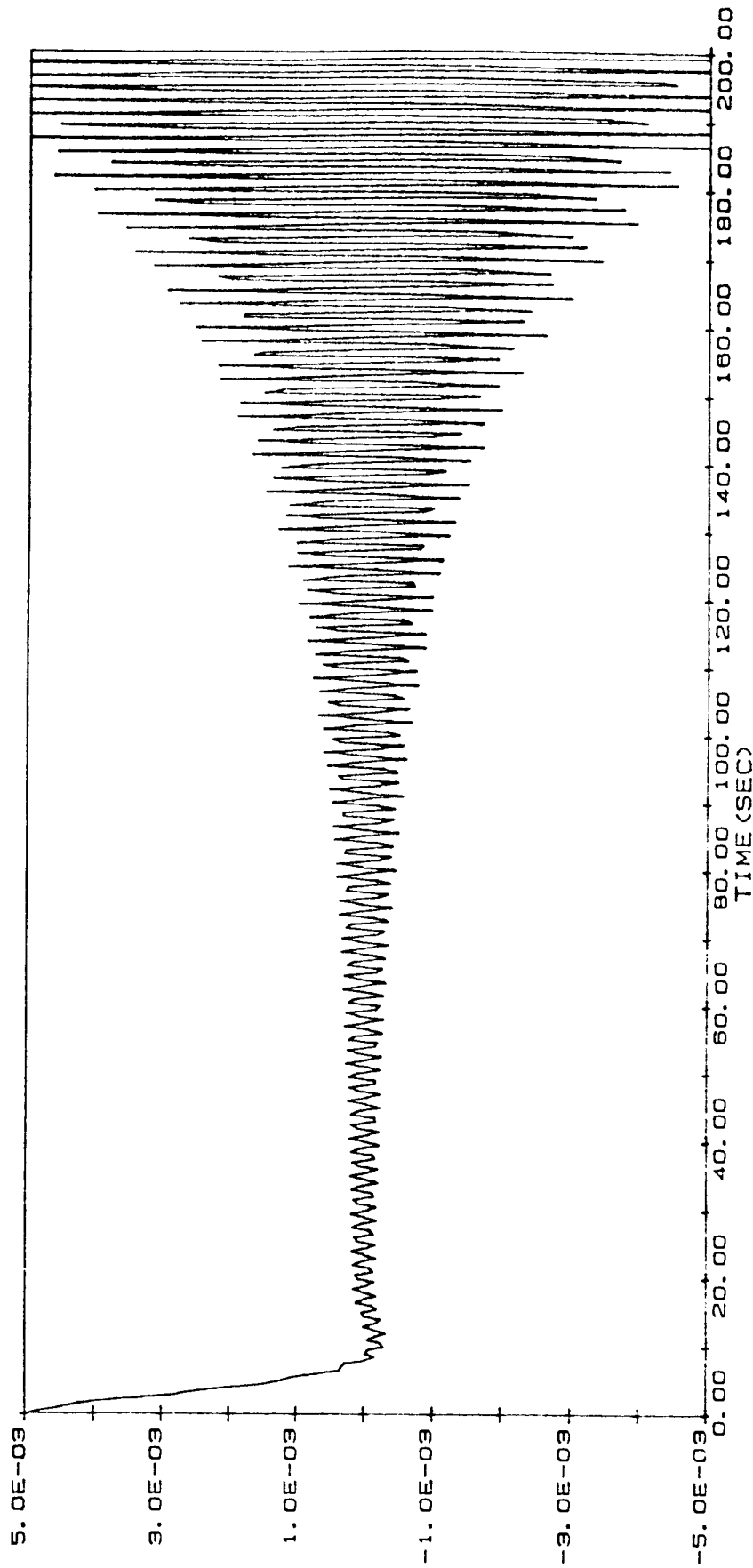


FIG A. 2-4 $\dot{\theta}_z$ -ANGULAR VELOCITY
GRAPH FOR VALUES CORRESPONDING
TO TRIAL #4-1-1
— ANGULAR VELOCITY (RAD/SEC)

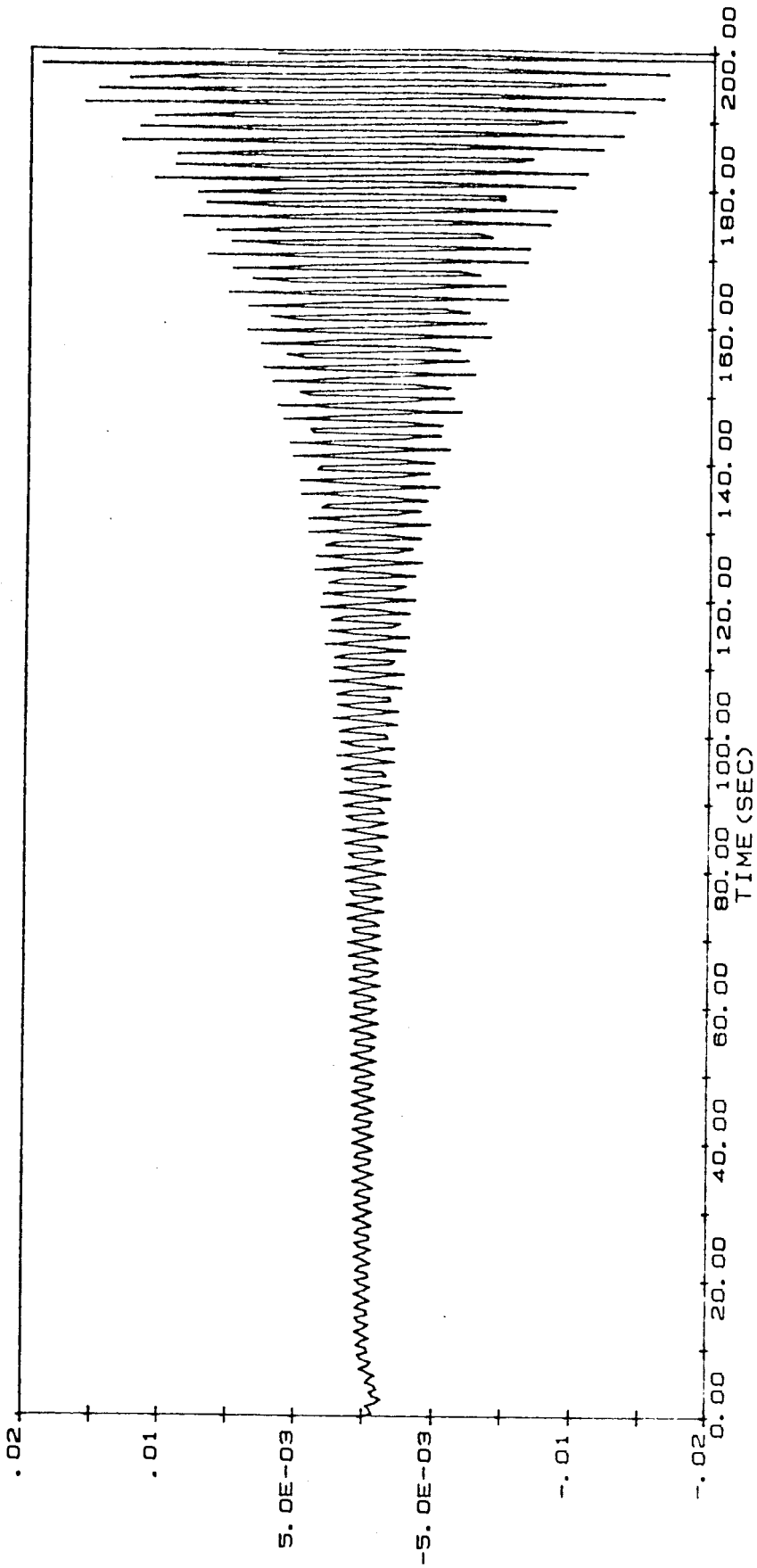


FIG A. 3-4 $\dot{\theta}_x$ -ANGULAR VELOCITY
GRAPH FOR VALUES CORRESPONDING
TO TRIAL #4-1-1
— ANGULAR VELOCITY (RAD/SEC)

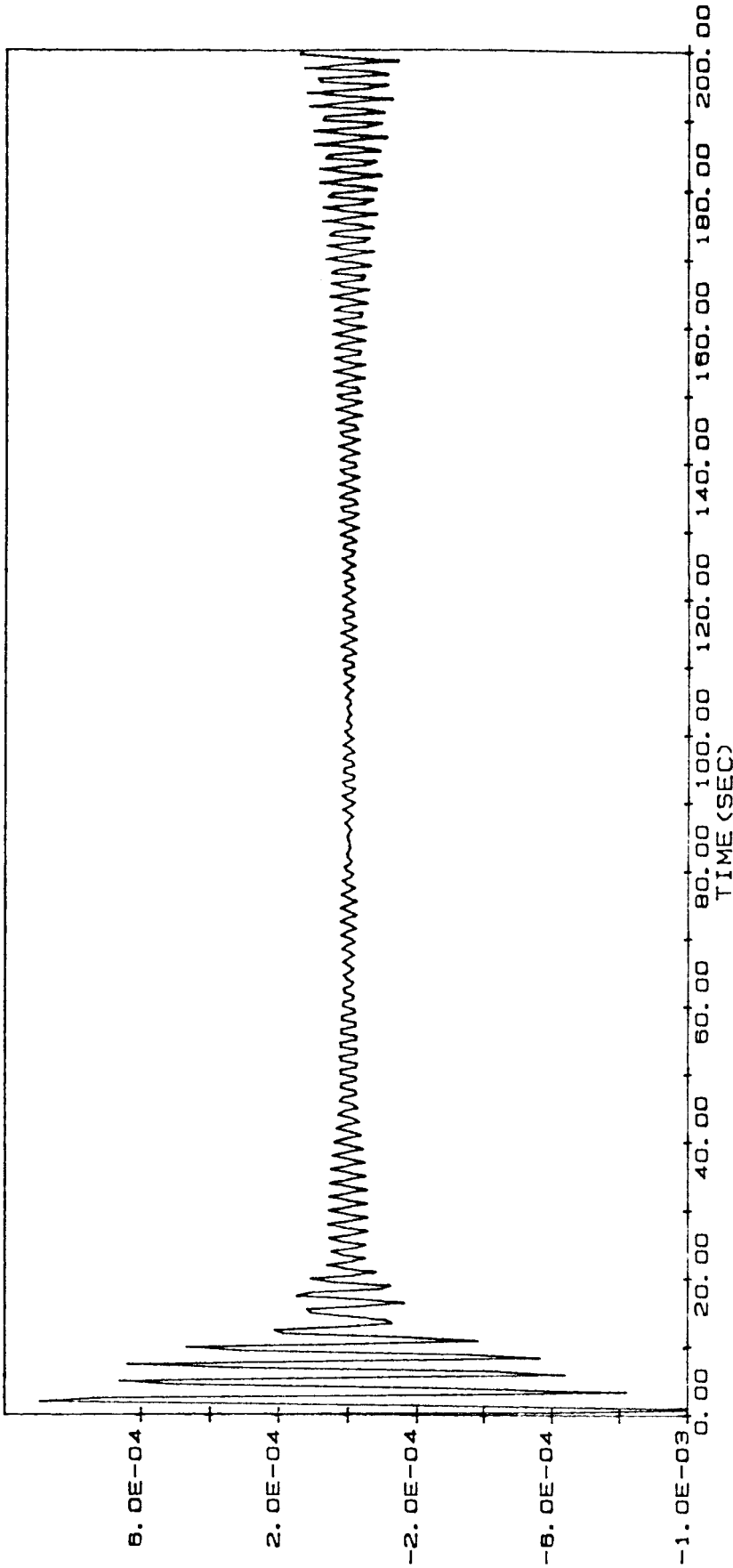


FIG A. 4-4 $\dot{\theta}_y$ -ANGULAR VELOCITY
GRAPH FOR VALUES CORRESPONDING
TO TRIAL #4-1-1
— ANGULAR VELOCITY (RAD/SEC)

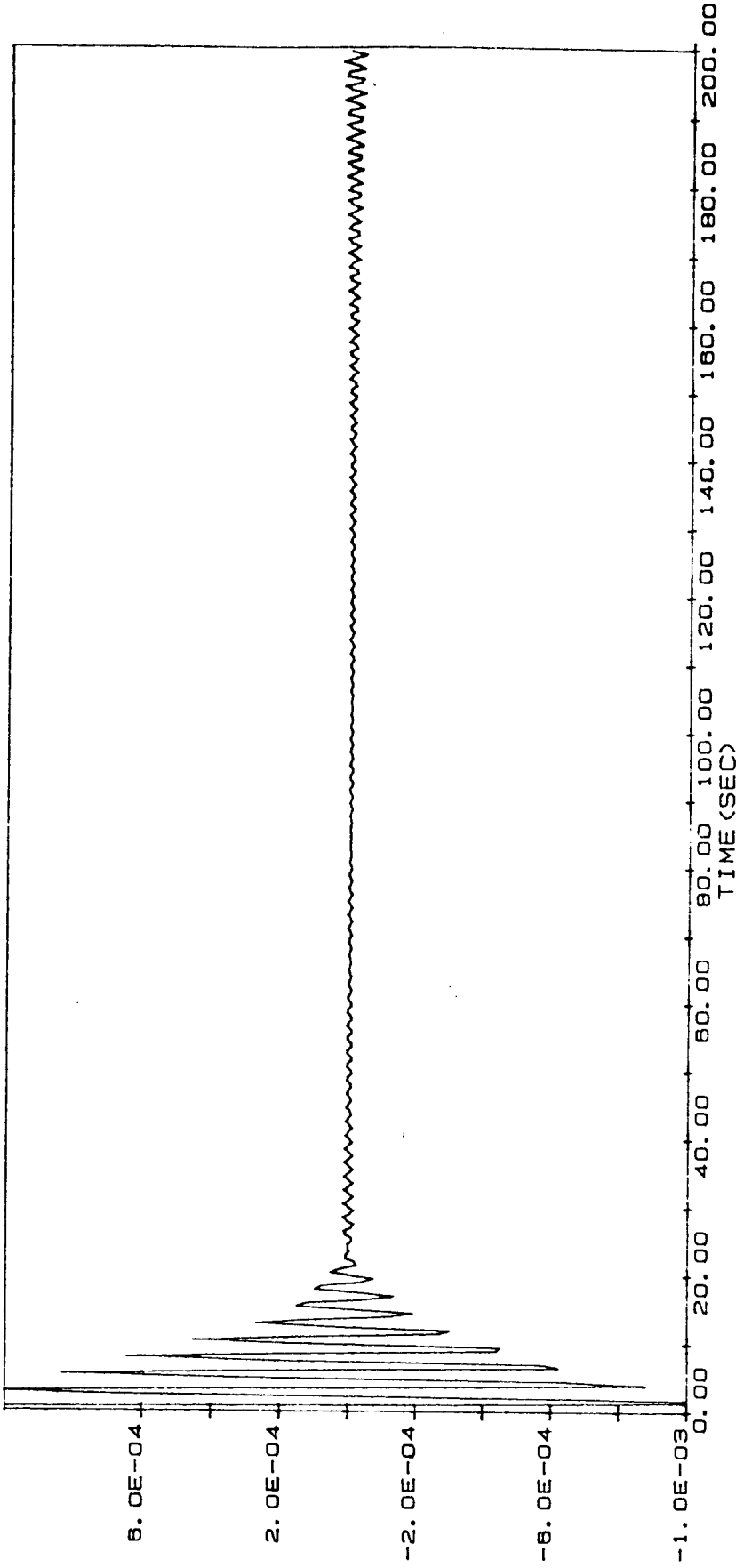


FIG A. 5-4 Q1-GEN. COORDINATE
GRAPH FOR VALUES CORRESPONDING
TO TRIAL #4-1-1
— GENERALIZED COORDINATE (q_i)

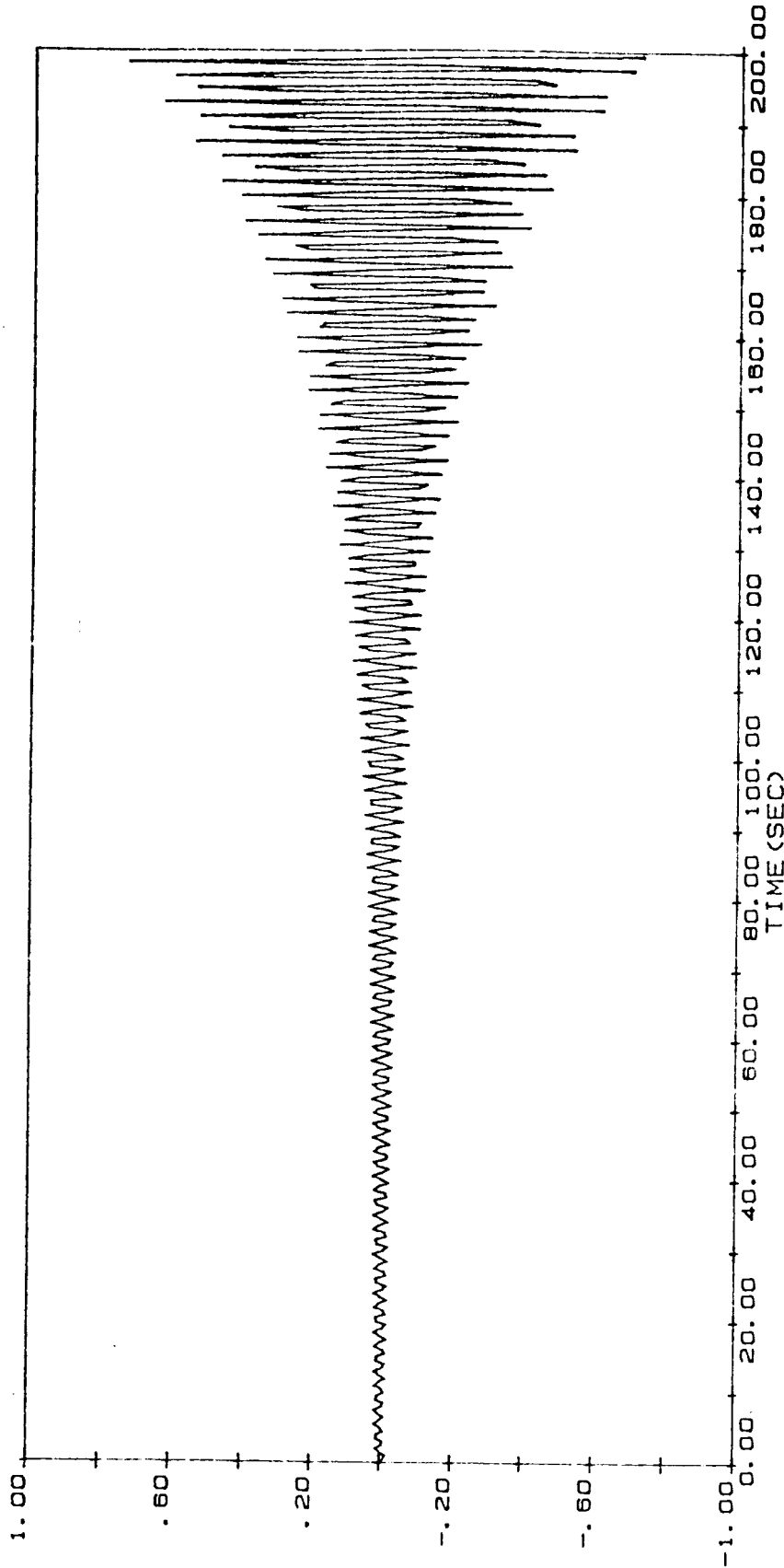


FIG A. 6-4 q2-GEN. COORDINATE
GRAPH FOR VALUES CORRESPONDING
TO TRIAL #4-1-1
GENERALIZED COORDINATE (q2)

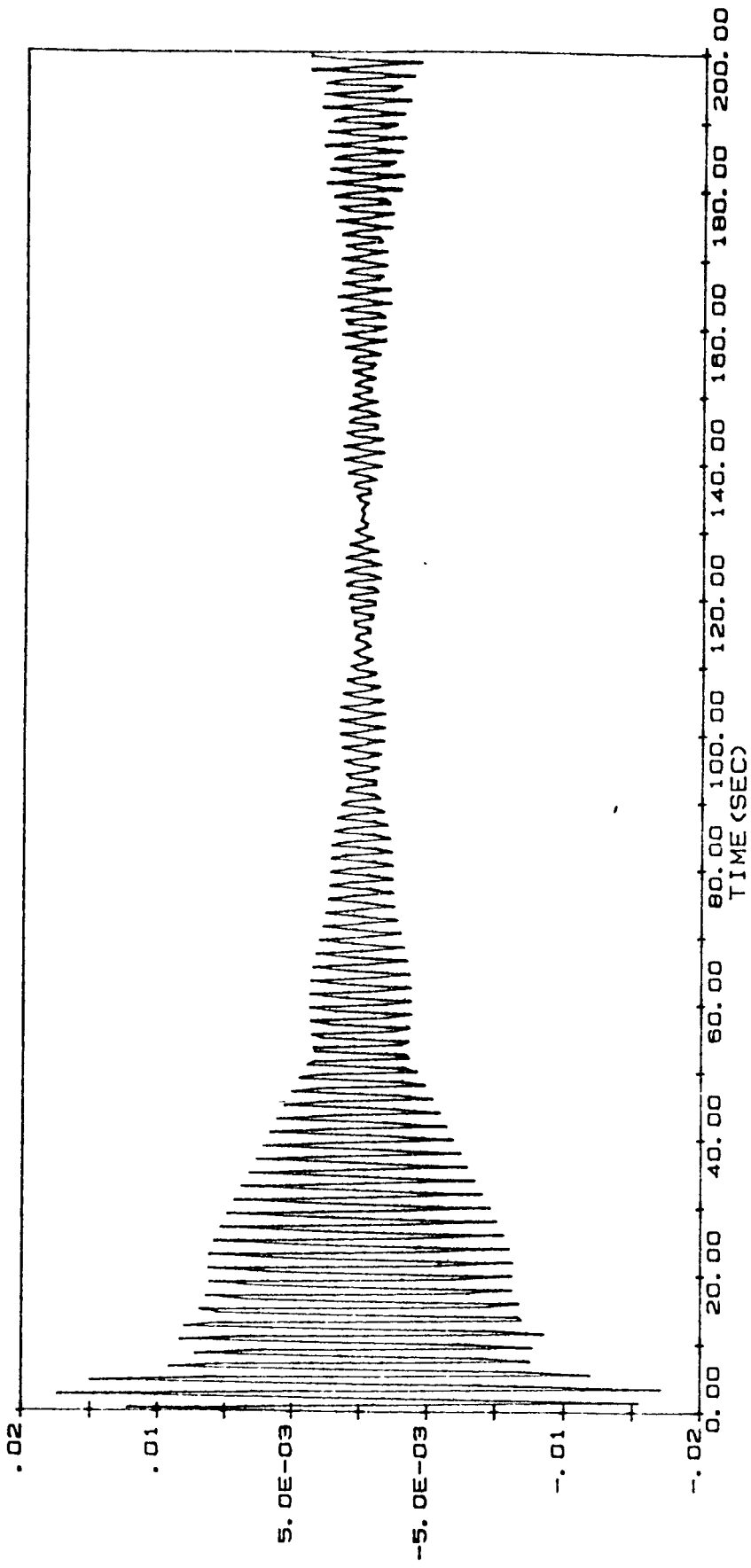


FIG A. 1-5 θ_z -ANGULAR DRIFT
GRAPH FOR VALUES CORRESPONDING
TO, TRIAL #5-1-1
— ANGULAR DRIFT (RAD.)

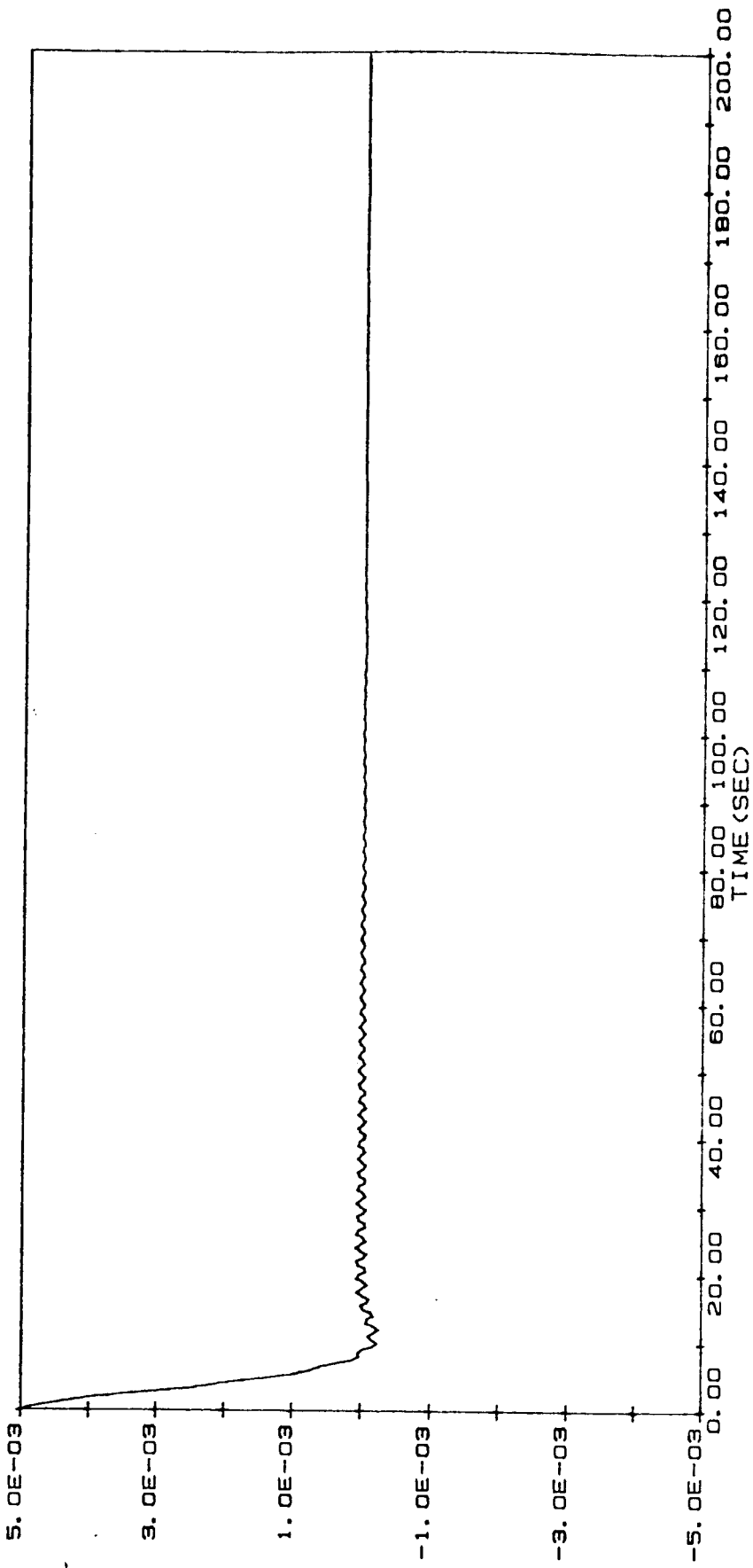


FIG A. 2-5 $\dot{\theta}_z$ -ANGULAR VELOCITY
GRAPH FOR VALUES CORRESPONDING
TO TRIAL #5-1-1
— ANGULAR VELOCITY (RAD/SEC)

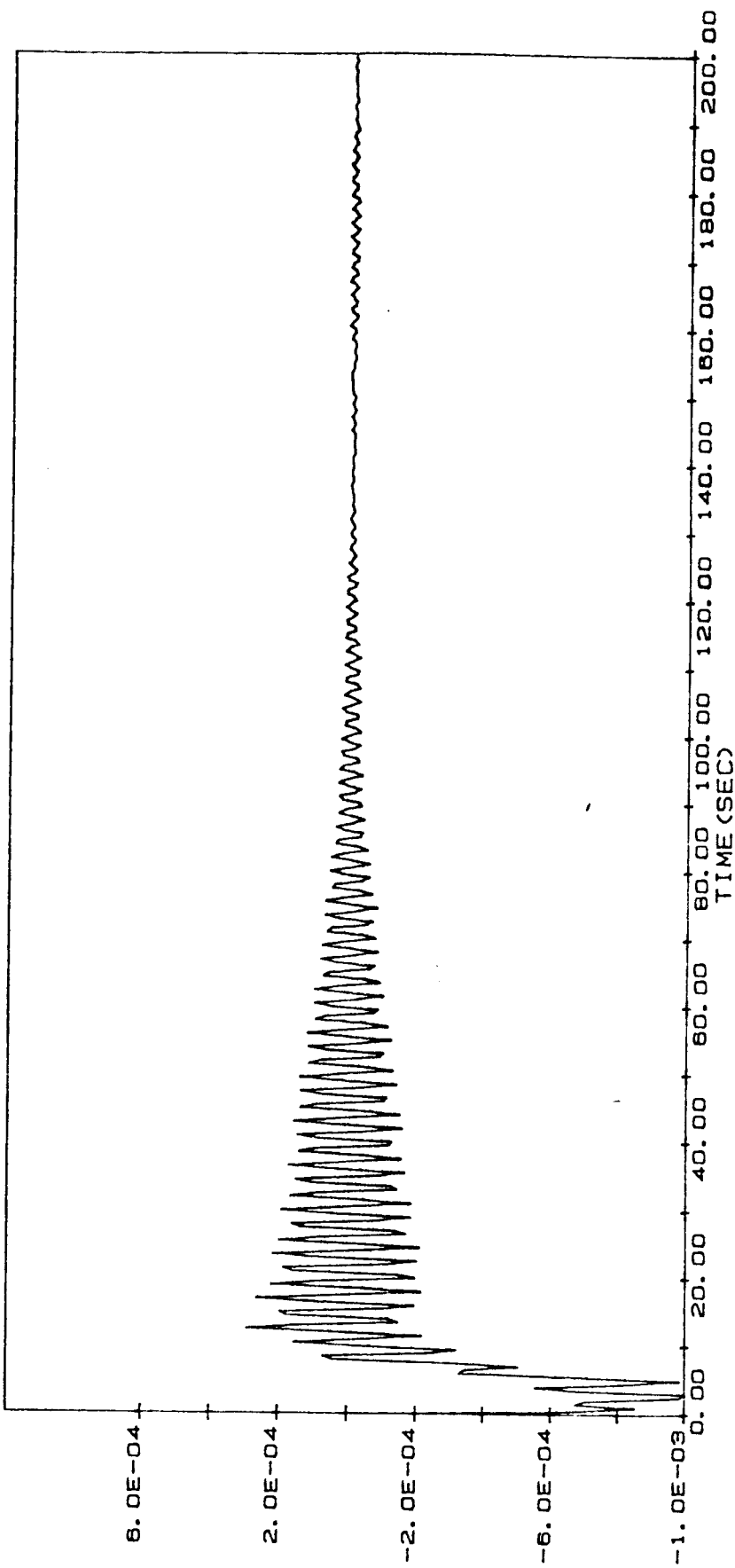


FIG A. 3-45 θ_x -ANGULAR VELOCITY
GRAPH FOR VALUES CORRESPONDING
TO, TRIAL #~~5~~1-1
— ANGULAR VELOCITY (RAD/SEC)

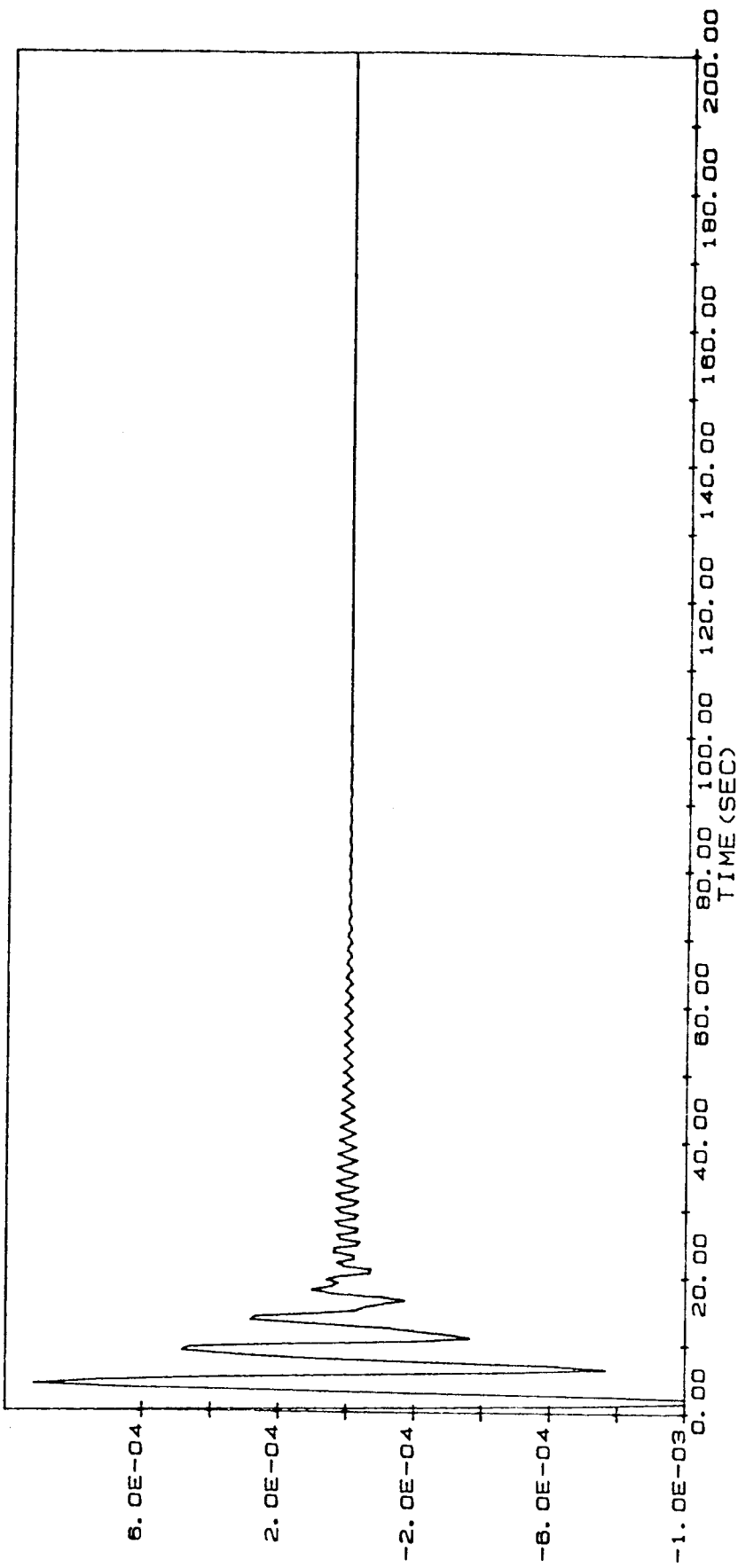


FIG A. 4-5 $\dot{\theta}_y$ -ANGULAR VELOCITY
GRAPH FOR VALUES CORRESPONDING
TO TRIAL #5-1-1
— ANGULAR VELOCITY (RAD/SEC)

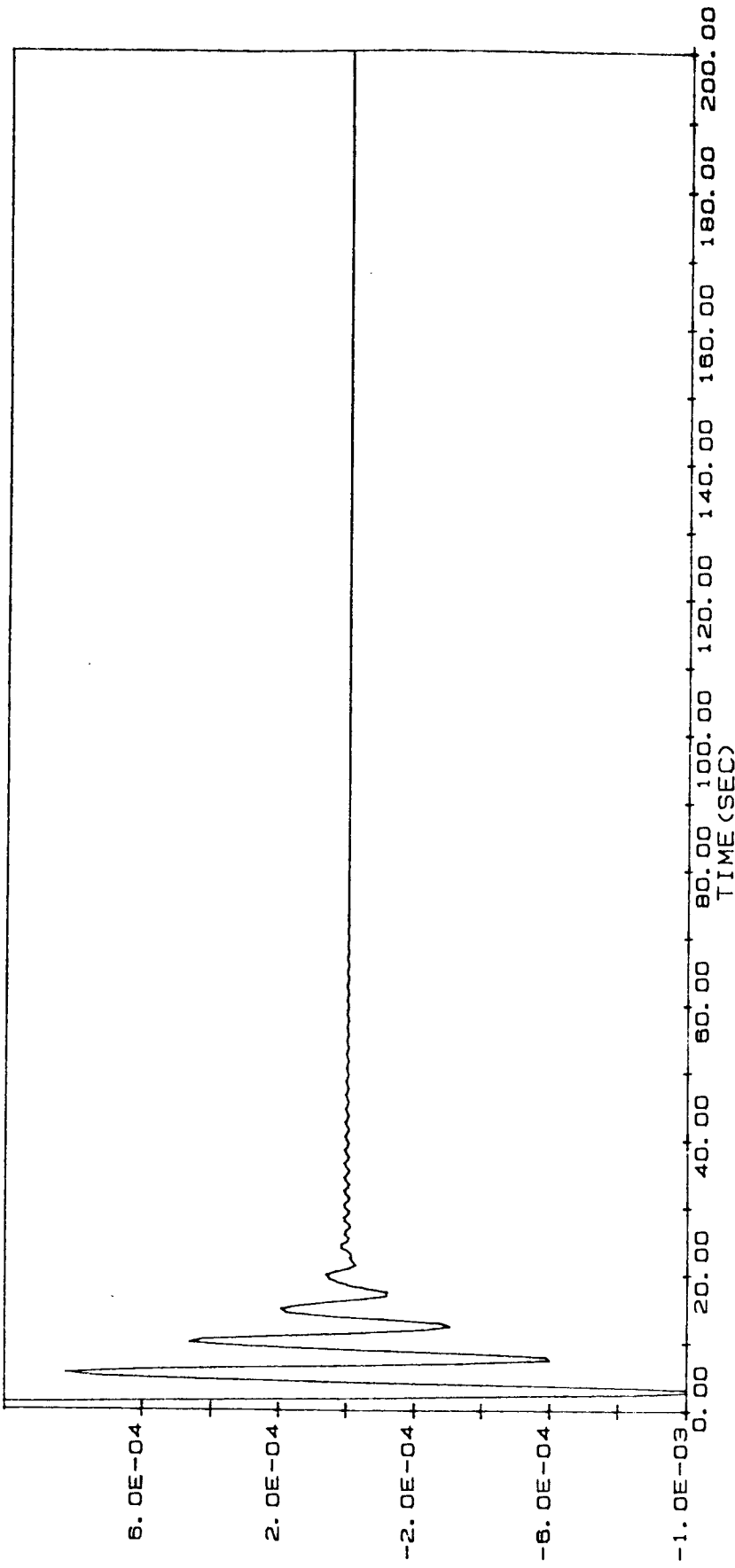


FIG A. 5-5 q₁-GEN. COORDINATE
GRAPH FOR VALUES CORRESPONDING
TO TRIAL #5-1-1
GENERALIZED COORDINATE (q₁)

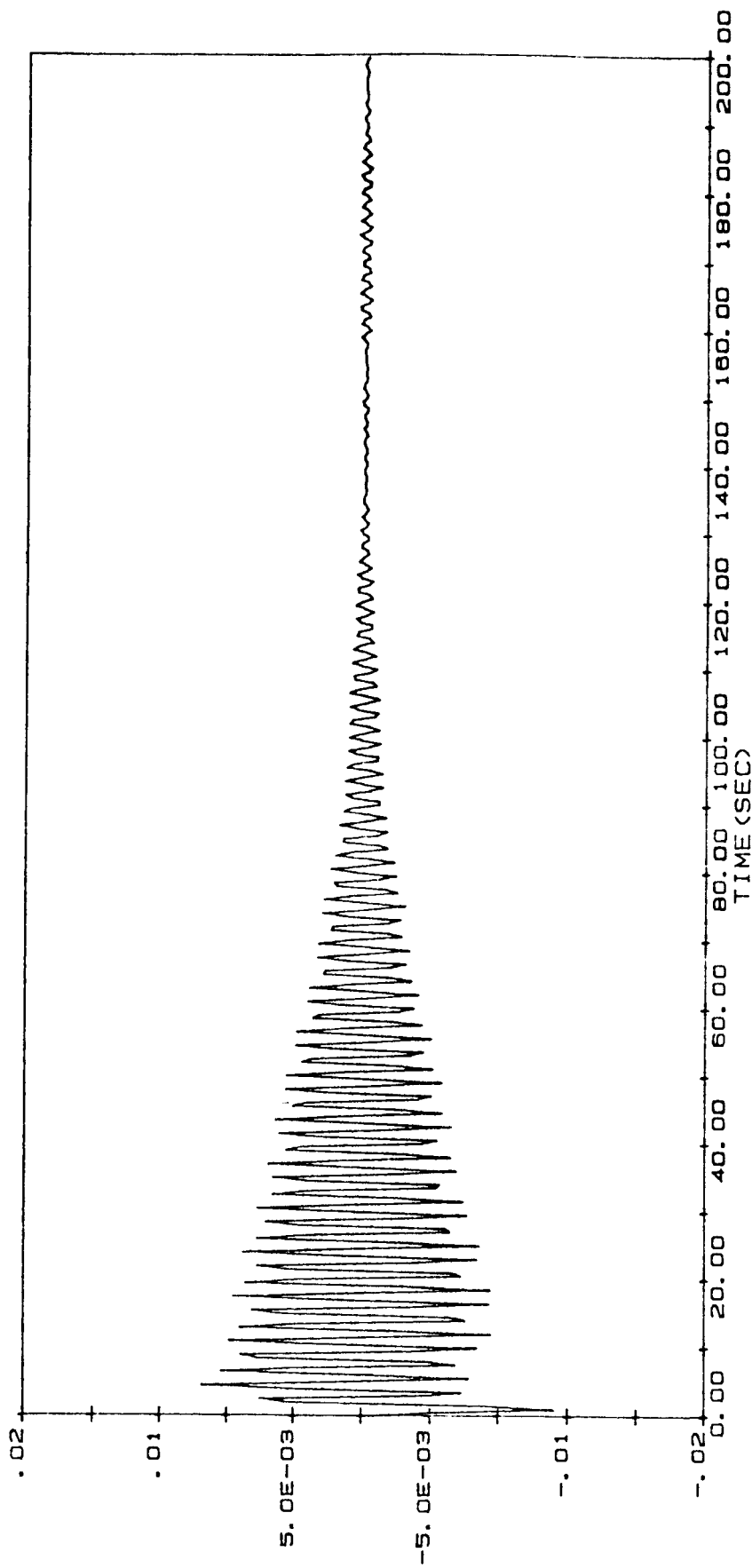


FIG A. 6-5 q2-GEN. COORDINATE
GRAPH FOR VALUES CORRESPONDING
TO TRIAL #5-1-1
GENERALIZED COORDINATE (q2)

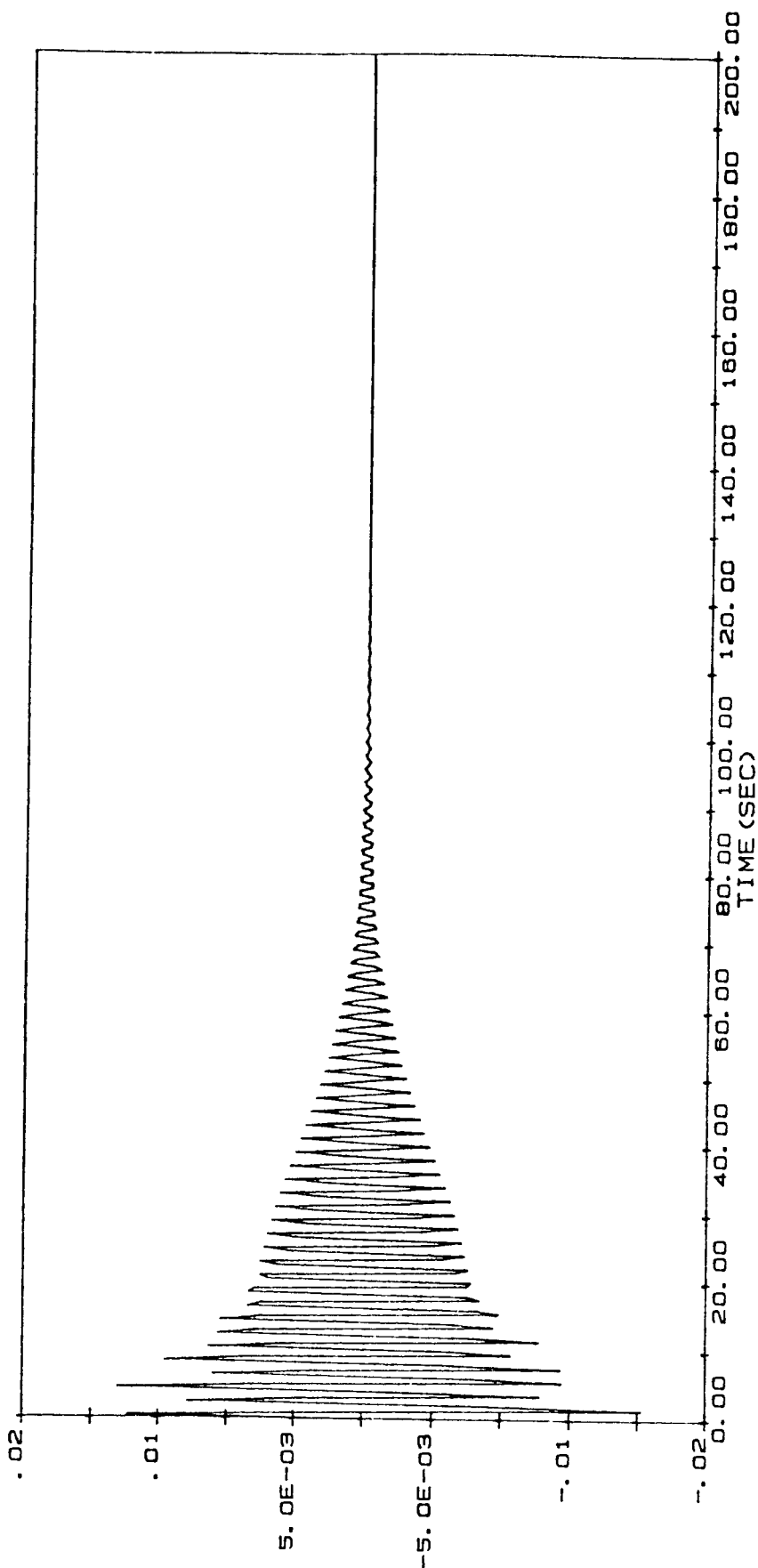


FIG A. 1-6 θ_z -ANGULAR DRIFT
GRAPH FOR VALUES CORRESPONDING
TO, TRIAL #1-2-2
— ANGULAR DRIFT (RAD.)

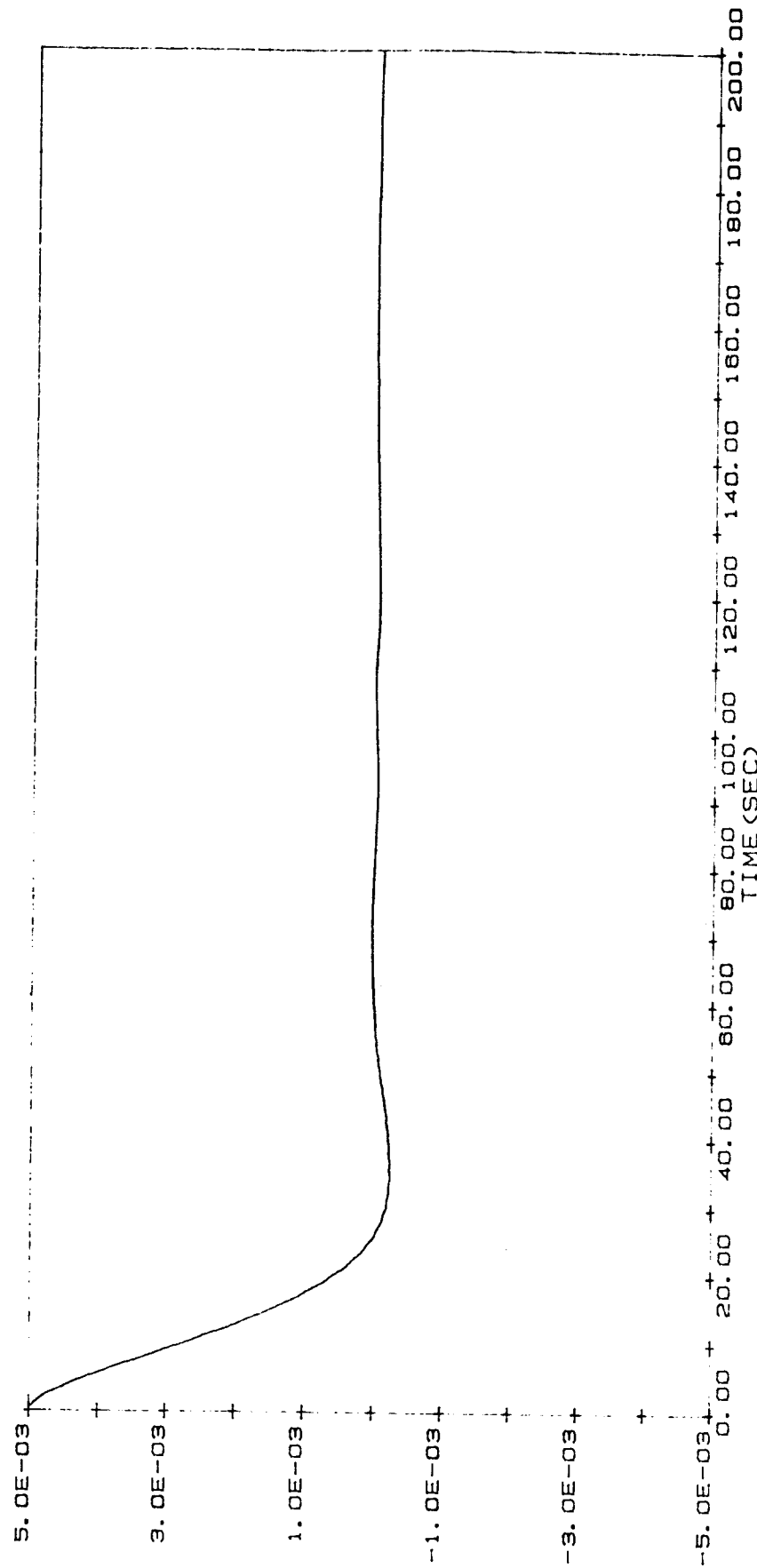


FIG A. 2-6 $\dot{\theta}_z$ -ANGULAR VELOCITY
GRAPH FOR VALUES CORRESPONDING
TO, TRIAL #1-2-2
— ANGULAR VELOCITY (RAD/SEC)

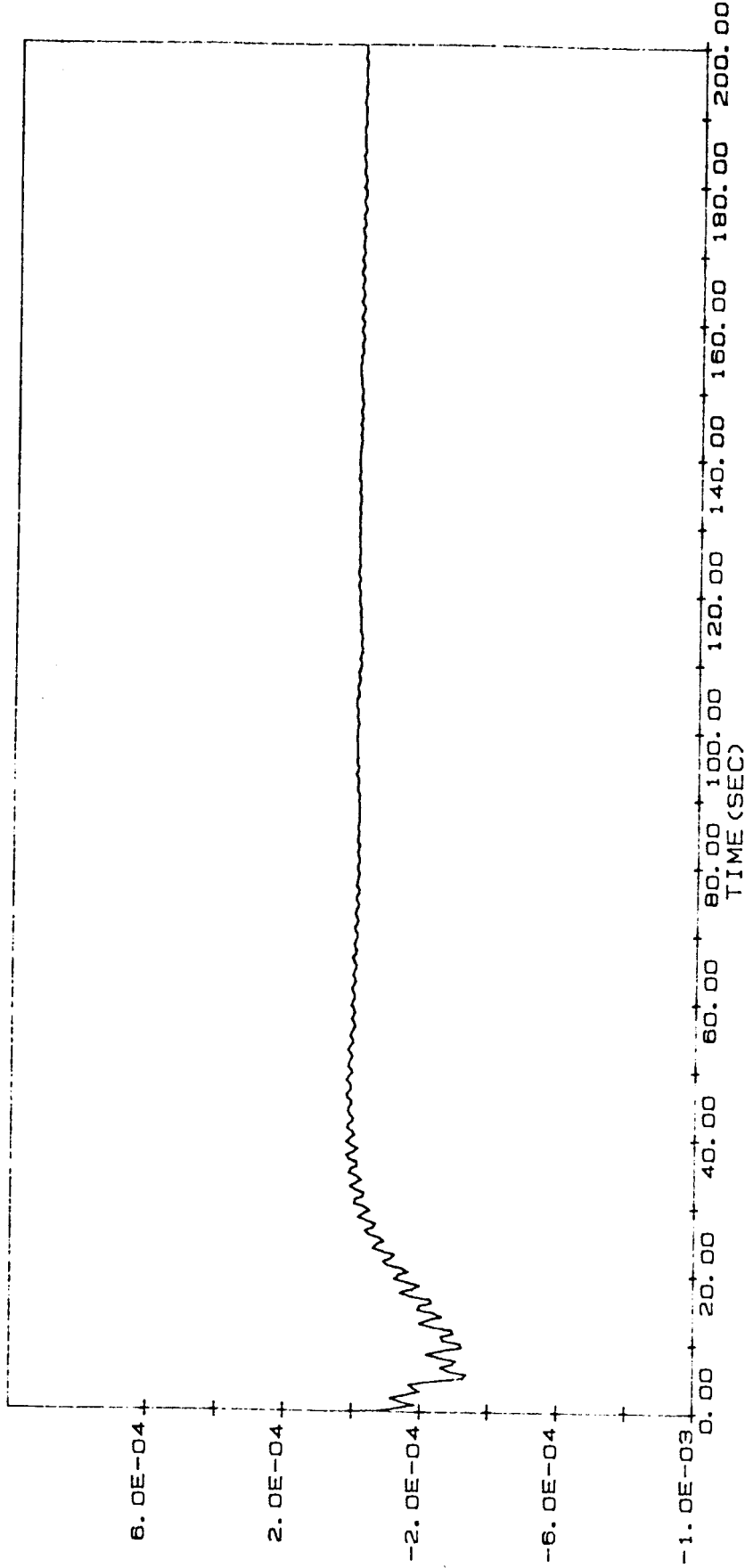


FIG A. 3-6 $\dot{\theta}_x$ -ANGULAR VELOCITY
GRAPH FOR VALUES CORRESPONDING
TO TRIAL #1-2-2
— ANGULAR VELOCITY (RAD/SEC)

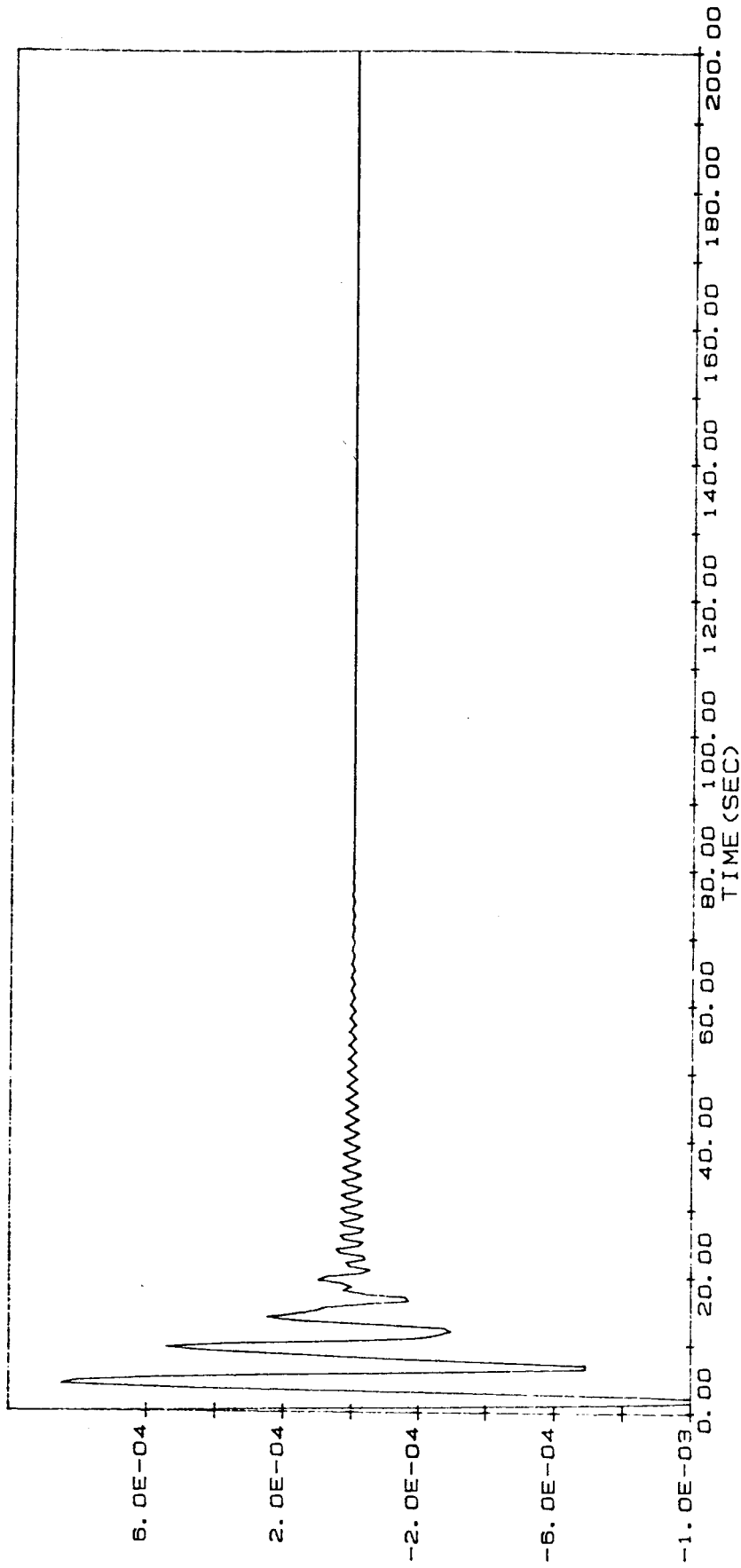


FIG A. 4-6 $\dot{\theta}_y$ -ANGULAR VELOCITY
GRAPH FOR VALUES CORRESPONDING
TO TRIAL #1-2-2
— ANGULAR VELOCITY (RAD/SEC)

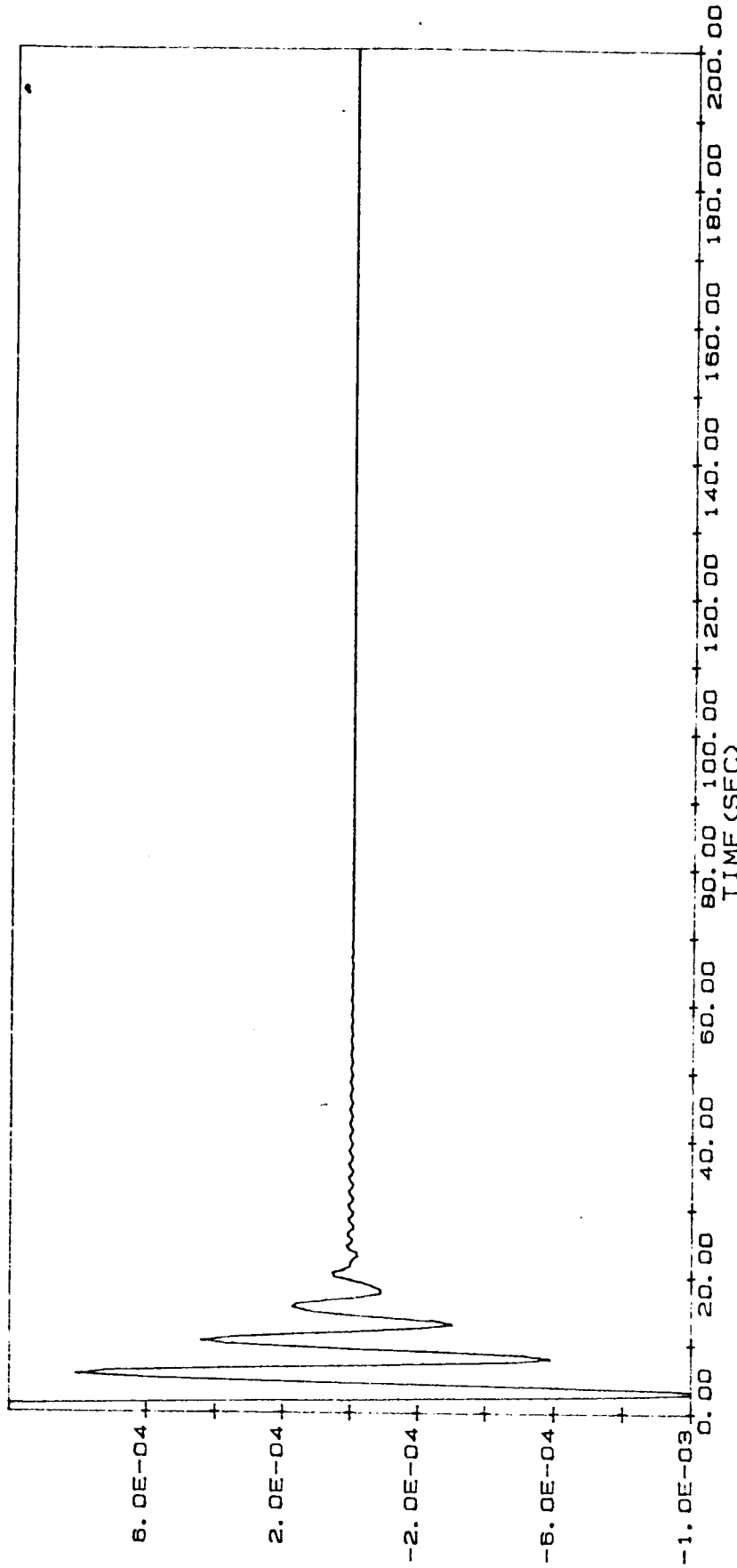


FIG A. 5-6 q1-GEN. COORDINATE
GRAPH FOR VALUES CORRESPONDING
TO TRIAL #1-2-2
— GENERALIZED COORDINATE (q1)

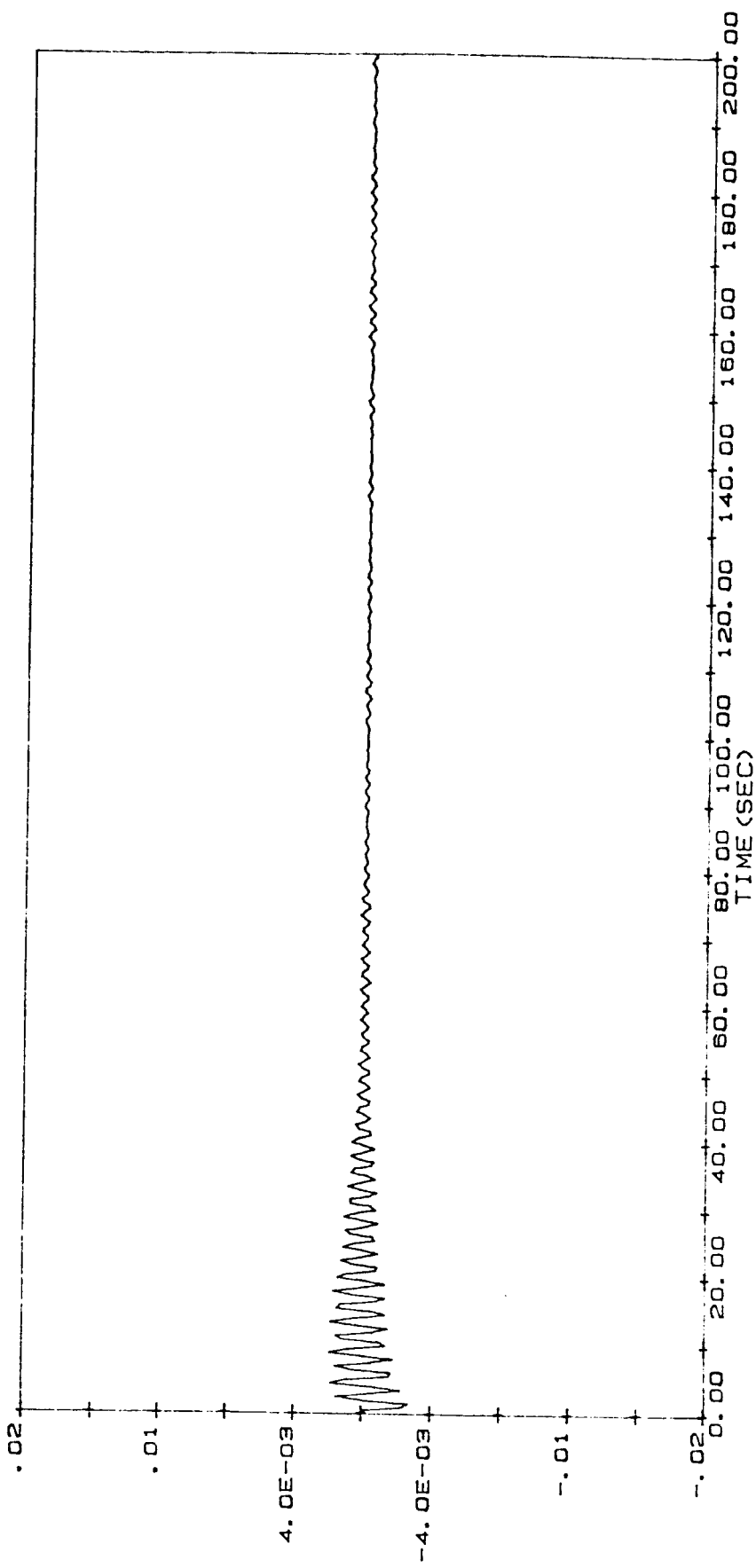


FIG A. 6-6 q2-GEN. COORDINATE
GRAPH FOR VALUES CORRESPONDING
TO TRIAL #1-2-2
GENERALIZED COORDINATE (q2)

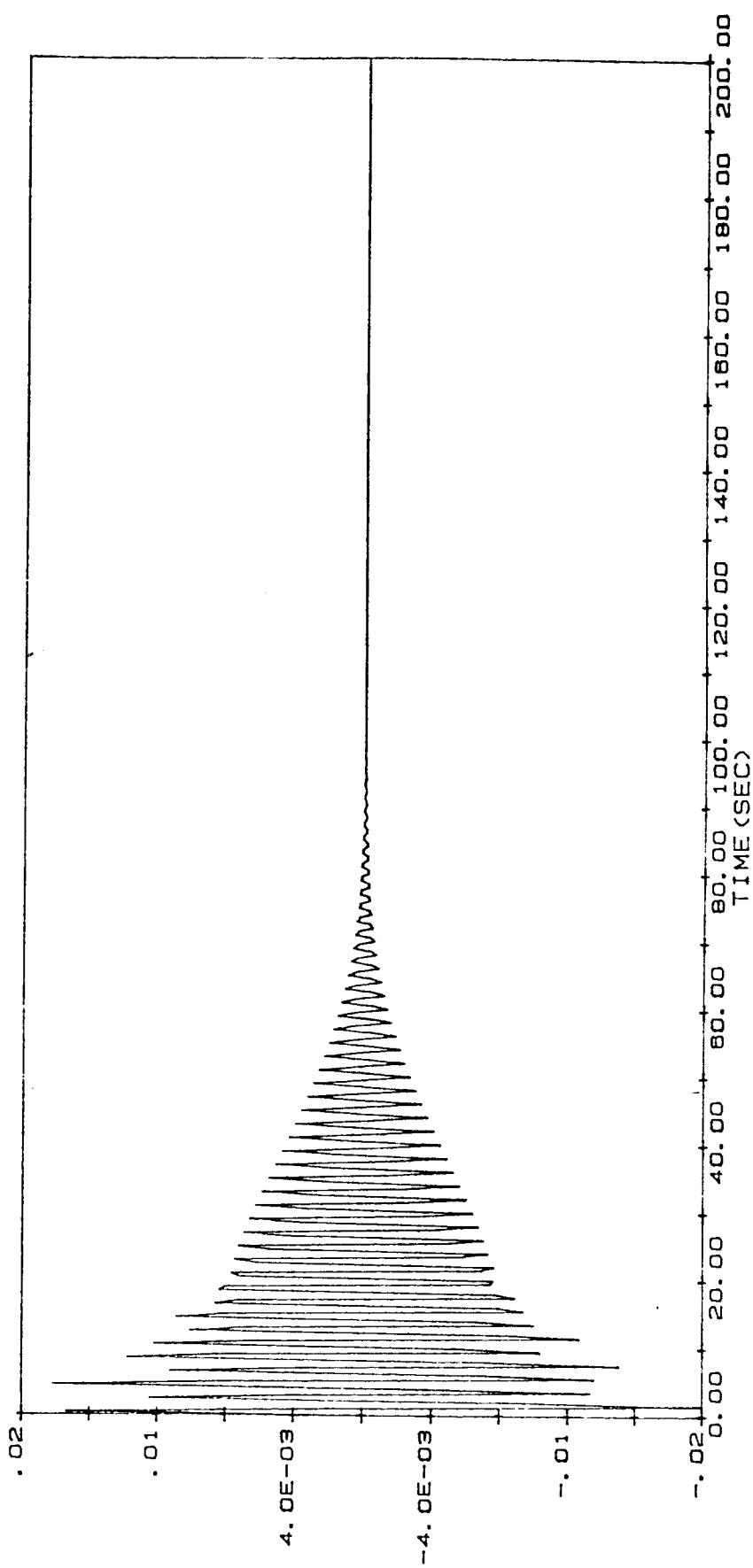


FIG A. 1-7 θ_z -ANGULAR DRIFT
GRAPH FOR VALUES CORRESPONDING
TO TRIAL #1-1-3
_____ ANGULAR DRIFT (RAD.)

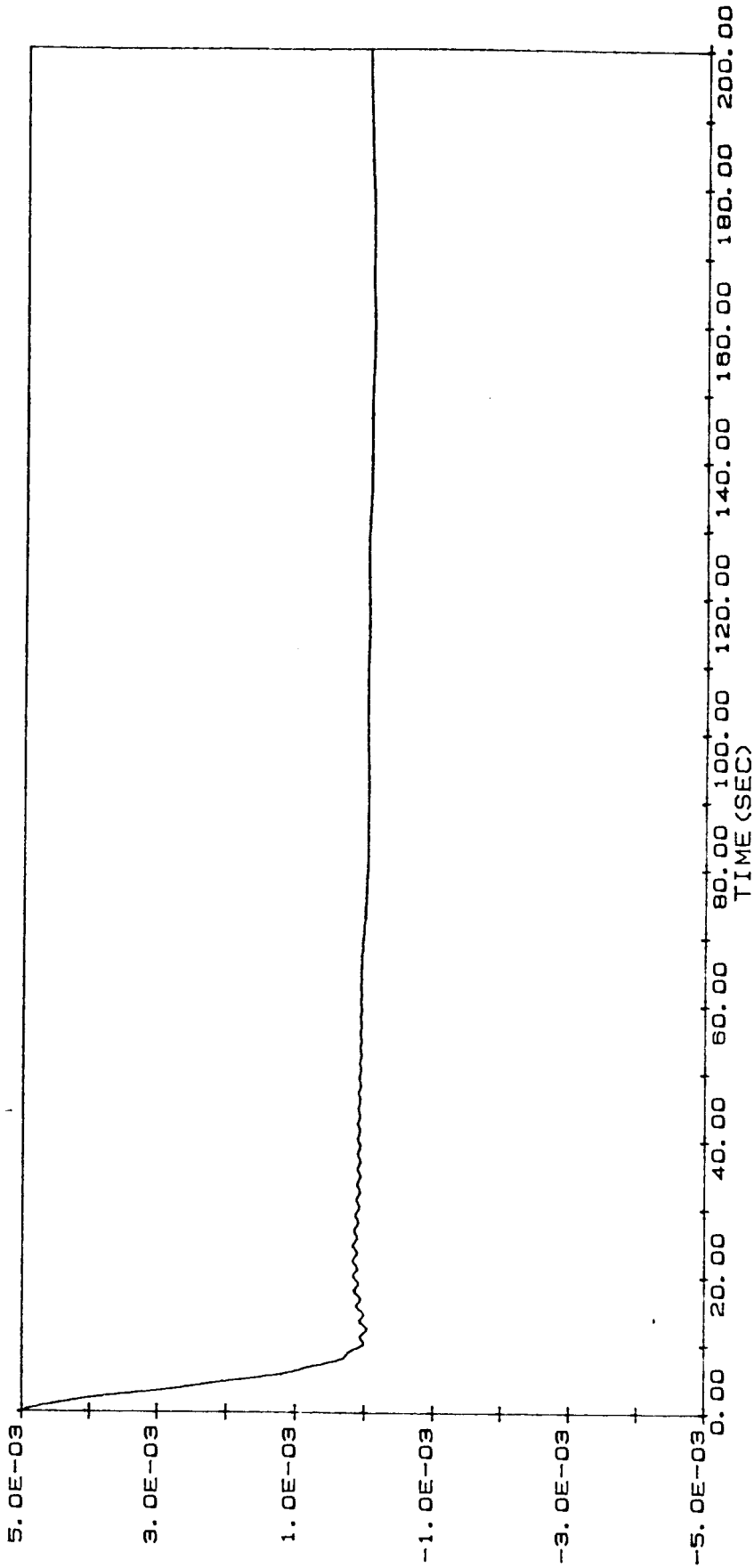


FIG A. 2-7 $\dot{\theta}_z$ -ANGULAR VELOCITY
GRAPH FOR VALUES CORRESPONDING
TO TRIAL #1-1-3
— ANGULAR VELOCITY (RAD/SEC)

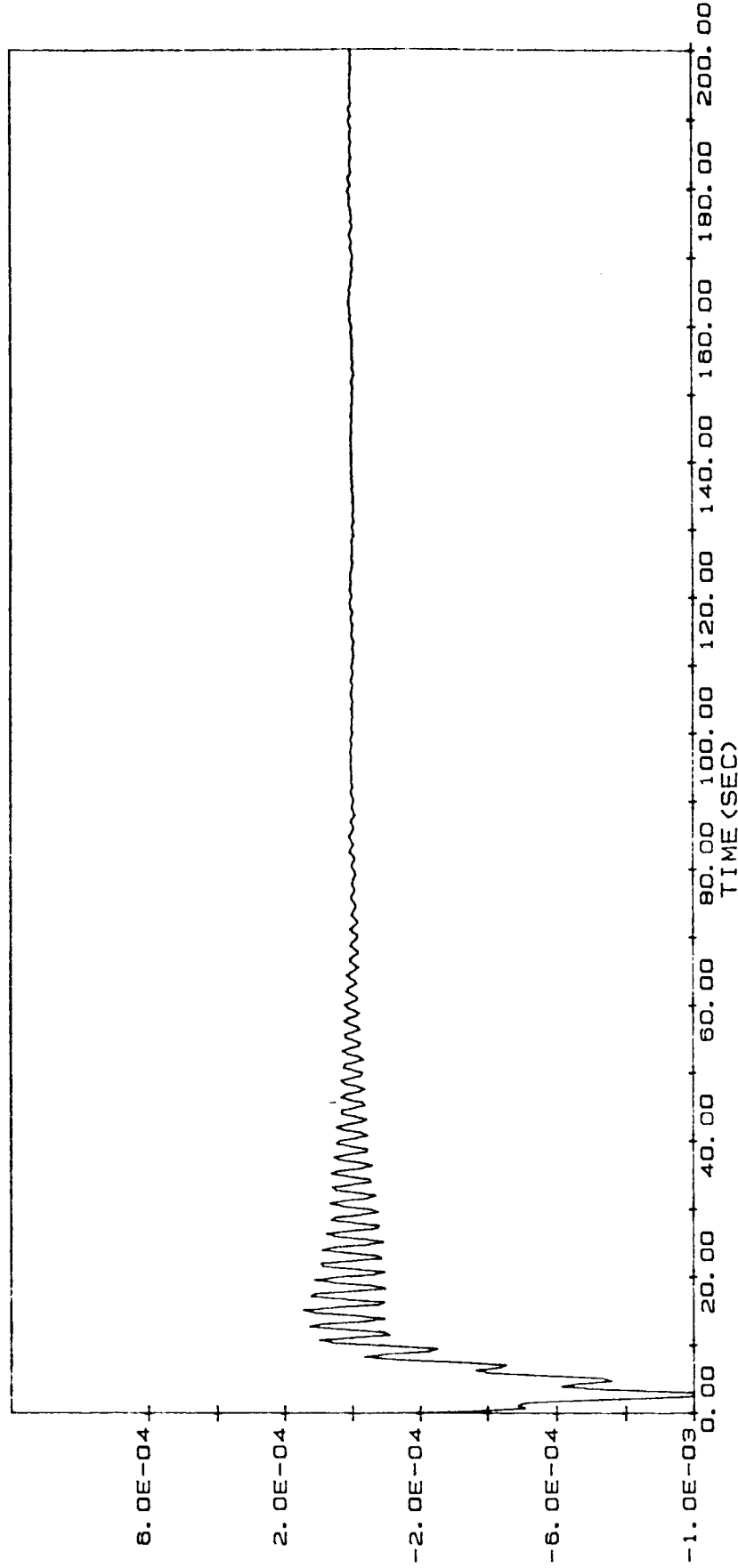


FIG A. 3-7 $\dot{\theta}_x$ -ANGULAR VELOCITY
GRAPH FOR VALUES CORRESPONDING
TO TRIAL #1-1-3
— ANGULAR VELOCITY (RAD/SEC)

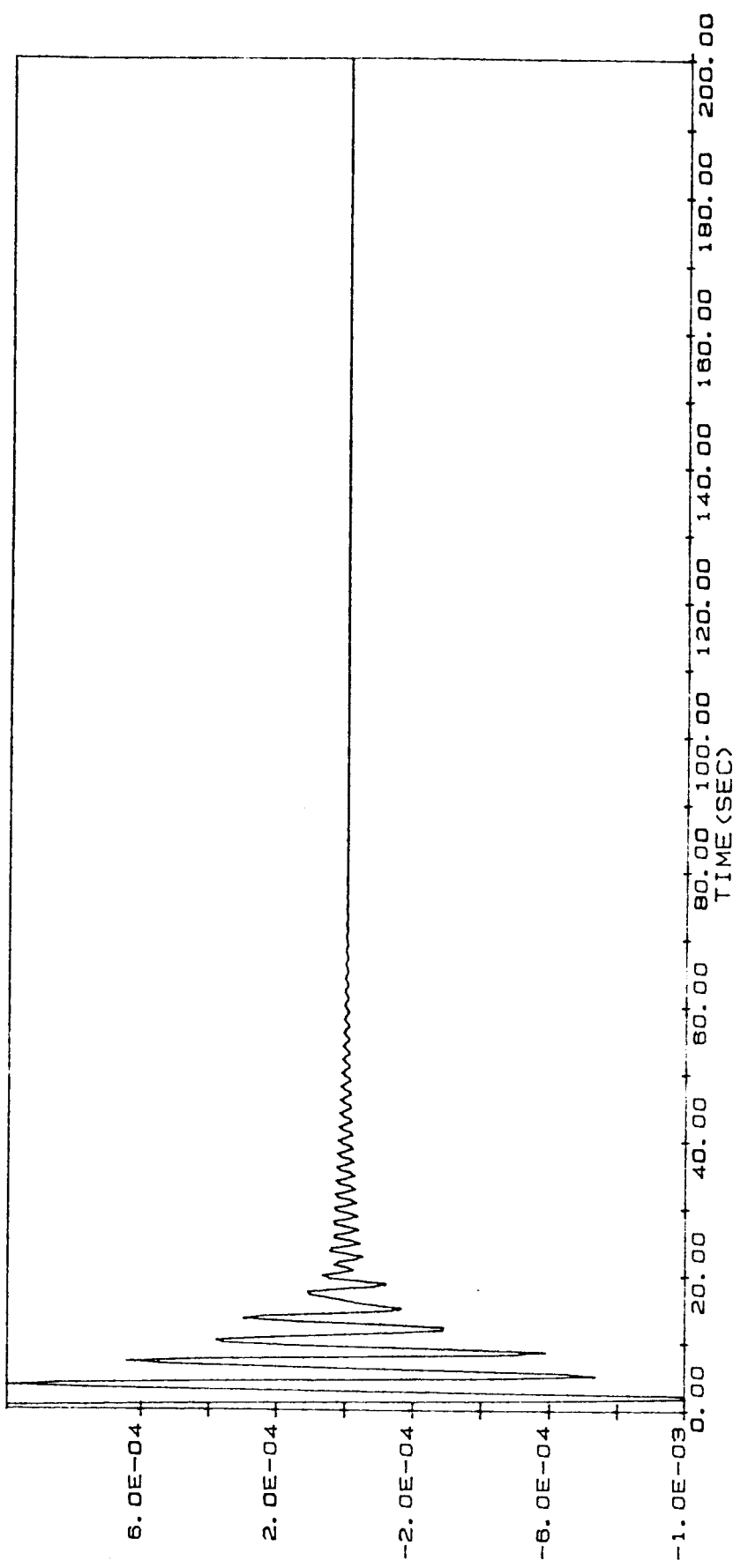


FIG A. 4-7 $\dot{\theta}_y$ -ANGULAR VELOCITY
GRAPH FOR VALUES CORRESPONDING
TO TRIAL #1-1-3
— ANGULAR VELOCITY (RAD/SEC)

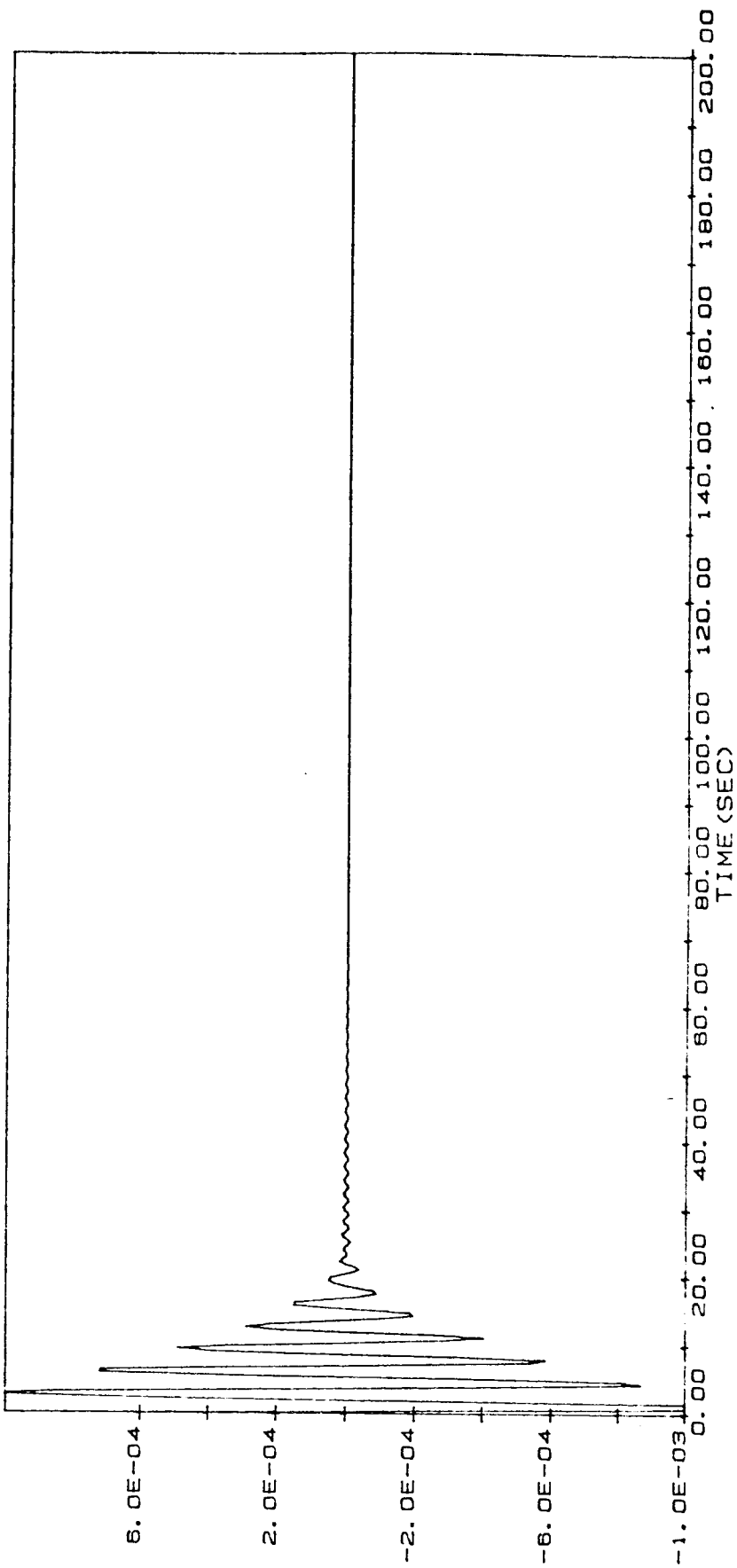


FIG A. 5-7 q1-GEN. COORDINATE
GRAPH FOR VALUES CORRESPONDING
TO TRIAL #1-1-3
GENERALIZED COORDINATE (q1)

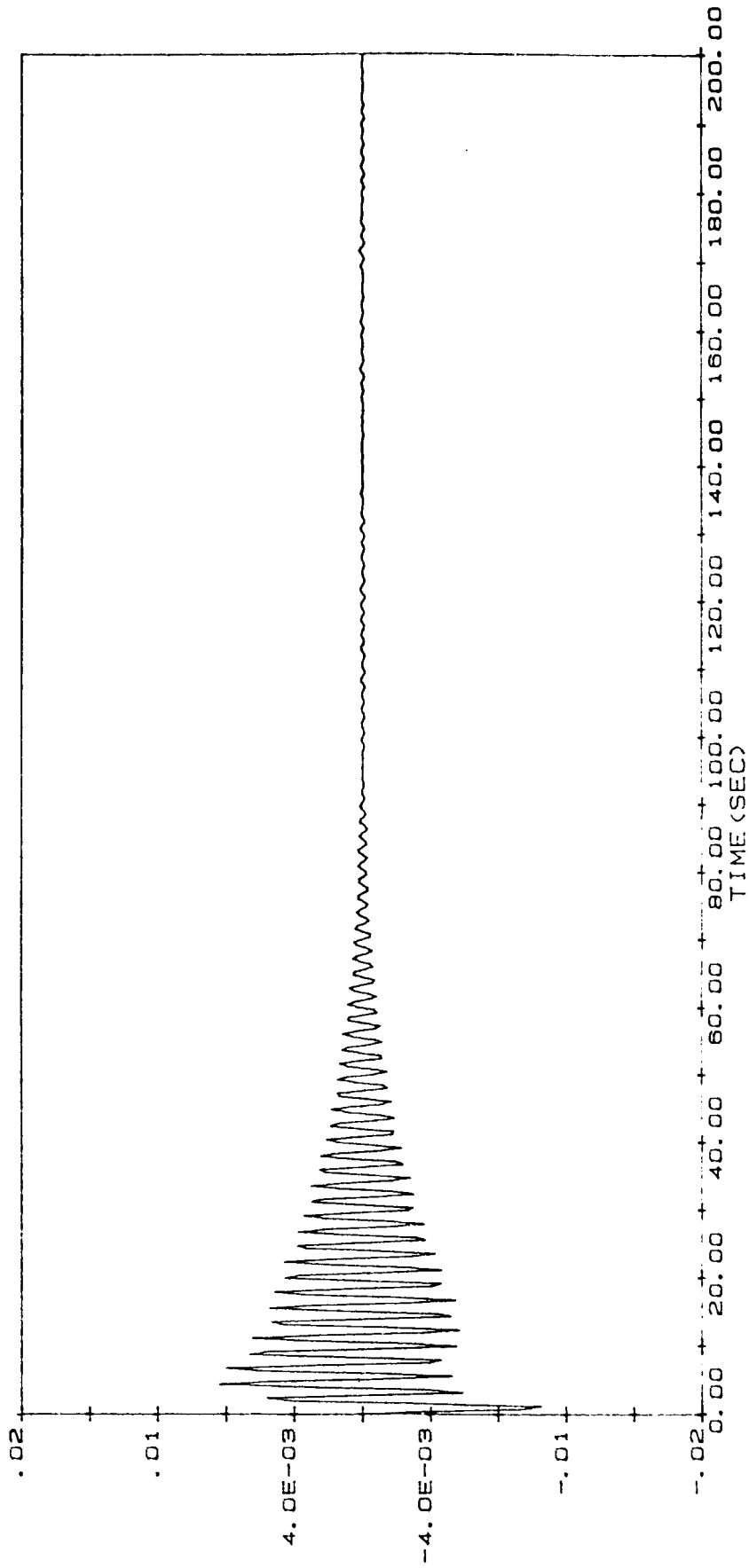


FIG A. 6-7 q2-GEN. COORDINATE
GRAPH FOR VALUES CORRESPONDING
TO TRIAL #1-1-3
— GENERALIZED COORDINATE (q2)

